Splenic follicular B cells promote adverse cardiac remodeling after myocardial infarction via MHC II-dependent antigen presentation.

Obialunanma V. Ebenebe PhD[1*], Jana P. Lovell MD[1*], Carolina Duque BS[2], Yiran Song MSc[1], Sylvie Rousseau BA[1], Kshipra Keole BA[1], Sogol Sedighi MD[1], Aashik Bhalodia BS[1], Kevin Bermea MD[1], Charles D. Cohen PhD[1], Monica R. Mugnier PhD[2], D. Brian Foster PhD[1], Scott Krummey MD PhD[3], Simone Sidoli PhD[4], Luigi Adamo MD PhD[1]

[1]Division of Cardiology, Department of Medicine, Johns Hopkins University School of Medicine, Baltimore, Maryland.
[2]W. Harry Feinstone Department of Molecular Microbiology and Immunology, Johns Hopkins Bloomberg School of Public Health
[3]Department of Pathology, Johns Hopkins University School of Medicine, Baltimore, Maryland
[4]Department of Biochemistry, Albert Einstein College of Medicine, Bronx, New York

*= these two authors share first authorship

Sources of Funding

This study has been funded through NHLBI grants 5K08HLO145108-03 and 1R01HL160716-01 to L.A. and T32-HL007227 to O.V.E and J.P.L and institutional funds from the Johns Hopkins Division of Cardiology awarded to L.A.

Disclosures

L.A. is co-founder of i-Cordis, LLC, a startup company focused on the development of immunomodulatory therapies for heart failure, and he is a consultant for Novo Nordisk and Kiniksa Pharmaceuticals.

Address of Correspondence:

Luigi Adamo, MD, PhD

Division of Cardiology
Johns Hopkins University School of Medicine
720 Rutland Avenue
Ross Research Building 809
Baltimore, MD 21205
Phone: 410-502-2857
Fax: 410-955-1962
@luigiadamomdphd

Abstract

The cardio-splenic axis is a promising therapeutic target in ischemic heart failure (HF), but splenic–cardiac interactions after myocardial infarction (MI) are poorly understood. Here, we show that splenic follicular B cells drive ischemic HF via MHC class II–mediated antigen presentation. Transfer of splenic B cells from mice with ischemic HF induced adverse cardiac remodeling and modulated myocardial T-cells in naïve recipients. Single-cell RNA sequencing of mouse and human post-MI B cells revealed upregulation of antigen-presentation related pathways. Mass spectrometry of the MHC II peptidome demonstrated enrichment of cardiac-derived peptides in MHC II molecules of splenic B cells from ischemic HF mice. B cell-specific deletion of MHC II suppressed adverse cardiac remodeling after adoptive transfer of post-MI splenic B cells. These results broaden our understanding of B-lymphocyte biology and point towards MHC II-mediated signaling in B-cells as a novel therapeutic target in ischemic HF.

54 Acute myocardial infarction (MI) triggers a robust activation of inflammatory responses [1, 2].
55 These inflammatory responses are physiological and necessary to limit tissue injury and induce
56 tissue repair [3, 4]. However, sustained inflammation contributes to adverse cardiac remodeling
57 and thus, to the development and progression of ischemic heart failure [5]. Despite advancements
58 in our understanding of the relationship between chronic inflammation and heart failure (HF),
59 clinical trials investigating immunomodulatory therapies in HF have yielded largely unsuccessful
60 results. The failure of these therapies is partly due to the inability to selectively target maladaptive
61 rather than protective inflammatory responses post-MI [6].
62
63 As such, an improved understanding of the sustained maladaptive inflammatory responses
64 contributing to the pathogenesis of chronic HF is needed. Prior murine and human data indicate
65 that acute MI induces splenic remodeling and mobilization of immune cells from the spleen to the
66 injured myocardium [7]. Activation of this "cardio-splenic axis" has been shown to contribute to
67 adverse cardiac remodeling and the development of chronic HF [8]. Thus, the cardio-splenic axis
68 has been identified as a promising therapeutic target for developing immunomodulatory treatments
69 for HF. However, our mechanistic understanding of the processes by which specific splenic
70 immune cells contribute to adverse cardiac remodeling remains limited.
71
72 B cells comprise the majority of immune cells within the spleen of most vertebrates. B cells are
73 also prevalent in healthy hearts and can recirculate between the spleen and the heart [9-11].
74 Growing evidence shows that B cells are intricately involved with cardiac function and
75 dysfunction, and following acute MI, contribute to the development and progression of ischemic

76 HF [12-16]. However, to date, the precise role of B cells within the cardio-splenic axis in HF has
77 not been systematically investigated.
78
79 Here, we show that B cells, specifically splenic follicular B cells, play an essential role within the
80 cardio-splenic axis of ischemic heart failure by promoting adverse cardiac remodeling post-MI via
81 MHC II-dependent antigen presentation.
82

83 **Results**

84 **Splenic B cells contribute to adverse cardiac remodeling in ischemic heart failure.**

85 To investigate whether splenic B cells are involved in the adverse cardiac remodeling of ischemic
86 HF, we designed adoptive transfer experiments. Unfractionated splenocytes or purified splenic B
87 cells were transferred from HF mice into naïve mice via intravenous injection. Splenic immune
88 cells isolated from sham-operated animals were used as controls. The naïve recipient mice were
89 monitored for eight weeks after adoptive transfer (Fig.1a).
90
91 Consistent with previously published data [8], we found that adoptive transfer of splenocytes from
92 mice with ischemic HF resulted in adverse cardiac remodeling in recipient mice. From serial
93 echocardiography, recipients of splenocytes from mice with HF had reduced left ventricular
94 ejection fraction (LVEF) and increased left ventricular end-systolic diameter (LVESD) eight
95 weeks post adoptive transfer compared to recipients of splenocytes from sham-operated mice
96 (Fig.1b; mean LVEF 68.1±1.7% vs 77.0±1.3% HF vs. sham recipient, $q<0.001$ at 8 weeks; mean
97 LVESD 2.01±0.7mm vs. 1.67±0.02mm HF vs. sham recipient, $q<0.001$ at 8 weeks).
98

99 To investigate the specific role of splenic B cells within the cardio-splenic axis following ischemic
100 myocardial injury, we performed adoptive transfer of purified splenic B cells from HF or sham-
101 operated mice (≈95% isolated B cell purity, Supplementary Fig.1). Over the 8-week period, the
102 adoptive transfer of isolated splenic B cells from mice with HF produced a degree of adverse
103 remodeling similar to that observed with the adoptive transfer of unfractionated splenocytes
104 (Fig.1b, bottom panels). Recipients of splenic B cells from mice with HF experienced a progressive
105 reduction in LVEF and progressive LV dilatation, detected at 4- and 8-weeks post adoptive transfer
106 (Fig.1b; mean LVEF 67.6±1.6% vs. 77.3±1.3% HF vs. sham recipient, $q<0.001$ at 8 weeks; mean
107 LVESD 2.00±0.05mm vs. 1.66±0.06mm HF vs. sham recipient, $q<0.001$ at 8 weeks). Further
108 experiments wherein we extended the post adoptive transfer monitoring revealed that this effect
109 was progressive to 16-weeks post adoptive transfer (Supplementary Fig.2).
110 Adverse cardiac remodeling in naïve recipients of splenocytes and splenic B cells isolated from
111 HF mice was further indicated by gravimetric analyses of the heart and spleen, as well as wheat-
112 germ agglutinin (WGA) staining of myocardial cross-sections. Gravimetric analysis revealed
113 increased splenic and cardiac mass in recipients of splenic B cells from mice with HF compared
114 to recipients of B cells from sham-operated mice 8 weeks following adoptive transfer (Fig.1c; for
115 purified splenic B cells: spleen mean 3.11±0.4 mg/g vs 2.59±0.2 mg/g, $p = 0.03$; heart mean
116 4.85±0.05 mg/g vs 4.60±0.2 mg/g, $p = 0.03$; Supplementary Fig.3 displays the combined
117 gravimetric data from multiple independent experiments). Furthermore, WGA staining of
118 myocardial cross-sections showed that increased heart mass was associated with cardiomyocyte
119 hypertrophy (Fig.1d; $p = 0.002$).
120

121 **Adoptively transferred splenic B cells are distributed between the spleen and heart.**

122 To investigate the dynamics of adoptively transferred splenic B cells, we repeated the adoptive
123 transfer experiments using animals carrying CD45.1 isoform as donors and animals carrying
124 CD45.2 isoform as recipients (Fig.2a). Donor CD45.1 B cells were present in the peripheral blood
125 of naïve recipient mice at 1- week and 8- weeks following adoptive transfer (Fig.2b; ~3% and ~2%
126 of circulating donor-derived B cells at 1- and 8- weeks, respectively). Flow cytometry of the spleen
127 and heart 8 weeks post-adoptive transfer also revealed the presence of donor CD45.1 B cells,
128 indicating successful engraftment of CD45.1 B cells in recipient mice (Fig.2b; Supplementary
129 Fig.4 also includes non-adoptive transfer controls).

130

131 **Ischemic myocardial injury results in differential expression of antigen processing and**
132 **presentation pathways in splenic B cells.**

133 To explore the mechanistic relationship between the adoptive transfer of splenic B cells from mice
134 with ischemic HF and adverse cardiac remodeling in naïve mice, we first analyzed the recipients'
135 spleen and heart via high-dimensional flow cytometry. At the splenic level, adoptive transfer of
136 splenic B cells from mice with ischemic HF did not affect the numbers of splenic lymphocytes or
137 the prevalence of B cell subsets (Fig.2c, Extended data Figure 1); nor were there changes in splenic
138 CD3 T cells, CD4 T cells, and CD8 T cells numbers relative to recipients from sham-operated
139 mice (Fig.2c). Closer examination of splenic T cell subsets indicated minor differences. We noted
140 a downward trend in the percentage of memory CD4 T cells expressing CTLA-4 and FOXP3
141 ($CD44^{hi}$, $CD62L^{lo}$, CTLA-4^{+}, $FOXP3^{+}$) and a corresponding increase in memory CD4 T cells
142 negative for CTLA-4 and FOXP3 markers ($CD44^{hi}$, $CD62L^{lo}$, CTLA-4^{-}, $FOXP3^{-}$, Extended Data
143 Fig.2). We did not detect differences in subsets of splenic CD8 T cells (Extended Data Fig.3). At
144 the myocardial level, via flow cytometry, we did not detect differences in cardiac immune cell

145 populations between recipients of splenic B cells from mice with ischemic HF and recipients of
146 splenic B cells from sham-operated mice (Extended Data Fig.4).
147
148 Since this analysis was unrevealing, we focused our attention on the donors; the population of
149 splenic B cells that were being adoptively transferred. We first used high-dimensional flow
150 cytometry. Within the spleen, B cells can be sub-classified based on specific cell markers [17, 18].
151 There were no changes in the percentage of splenic B cell subtypes isolated from mice with
152 ischemic HF (4 weeks post-MI surgery) compared to sham-operated mice (Extended Data Fig.5).
153 We then used single-cell RNA sequencing (scRNAseq) to more deeply probe the molecular
154 character of the donor splenic B cells from HF mice (Fig.3a). V(D)J analysis did not reveal an
155 expansion of specific splenic B cell clonotypes in ischemic HF (4 weeks post-MI). Suggesting that
156 the effects observed at the time of adoptive transfer were not due to splenic B cells' clonal
157 expansion (Fig.3b; Supplementary Fig.5). UMAP plots were then used to visualize the clustering
158 of gene expression profiles of splenic B cells (Fig.3c). Comparative gene expression analysis
159 revealed several genes differentially expressed in splenic B cells from mice with ischemic HF (4
160 weeks post-MI surgery) (Supplementary Table 1).
161 To evaluate the biological relevance of these differentially expressed genes (DEGs), we performed
162 pathway analyses using KEGG pathway annotation [19, 20]. Antigen processing and presentation
163 was the top biological pathway identified as differentially regulated (q-value = 8.02E-9; Fig.3d).
164 Some of the specific DEGS included HSPA8, HSP90AA1, HSP90AB1, which encode heat shock
165 proteins (HSPs) involved in MHC-II mediated antigen presentation [21, 22]; H2-Eb1 and H2-
166 DMb1 which encode MHC-II proteins and IFI30 (also known as GILT) which is involved in MHC-
167 II mediated antigen presentation [23]. Further evaluation of B cell subtypes revealed significant

168 differential regulation of the antigen processing and presentation pathway in the follicular,
169 germinal center, regulatory, plasma, and memory B cells (Fig.3d) but not in marginal zone B cells
170 (Supplementary Table 2).
171
172 To further corroborate these findings, we expanded our analysis to myocardial B cells and
173 peripheral blood B cells in animals with ischemic HF (Supplementary Figs.6 and 7). We also
174 included animals with recent MI (four days post-MI surgery) to gain longitudinal insight
175 (Supplementary Figs.8-10). These analyses also pointed towards antigen processing and
176 presentation as one of the top sustained, differentially regulated pathways in myocardial and
177 circulating B cells in response to myocardial injury. More specifically, antigen processing and
178 presentation was differentially regulated in multiple cardiac and peripheral blood, B cell subtypes
179 from mice with ischemic HF (Supplementary Figs.6 and 7), with an especially strong signal in
180 myocardial and circulating follicular B cells (Supplementary Figs.6C and 7C). Recent MI was
181 compared to the 8-weeks post sham surgery (which is a suboptimal control); yet this analysis also
182 highlighted significant differential regulation of antigen processing and presentation in splenic,
183 cardiac, and peripheral blood B cells with a predilection for follicular B cells (Supplementary
184 Figs.8-10). Lists of the DEGs associated with antigen processing and presentation in mice with
185 ischemic HF and mice with recent MI are provided within the spreadsheets included in
186 Supplementary Table 1.
187

188 **MHC II molecules of splenic B cells from mice with ischemic HF are loaded with cardiac**
189 **peptides.**

190 Collectively, our transcriptomic data suggested that splenic B cells might modulate adverse cardiac

191 remodeling in ischemic HF via major histocompatibility complex class II (MHC II) mediated
192 antigen presentation. This was an unexpected finding. B cells have three main functions: antibody
193 production, cytokine secretion, and antigen presentation. It has been reported that B cells may
194 contribute to adverse cardiac remodeling following MI via the production of autoantibodies or
195 chemokine-mediated mobilization of monocytes from the spleen to the heart [12, 24]. However,
196 to our knowledge, B cell-mediated antigen presentation has never been implicated in the
197 pathogenesis of cardiac dysfunction. To further investigate the potential role of MHC II-mediated
198 antigen presentation in ischemic myocardial injury, we isolated MHC II-associated peptides from
199 splenic B cells of sham-operated and ischemic HF mice (4 weeks post-MI) and analyzed them via
200 mass spectrometry (Fig.3e). Peptides enriched more than 1.2-fold in MHC II molecules from post-
201 MI B cells were analyzed *in silico* with a software that predicts peptide binding to the MHC II
202 isoform expressed on C57BL/6 mice. 54 enriched peptides were identified as predicted binders in
203 the *in-silico* analysis, corresponding to 45 proteins. 18% of these proteins were cardiac-specific
204 (Fig.3f). 13 peptides were predicted as strong binders. These included several cardiac-specific
205 proteins such as cardiac α actin (ACTC1), Titin (TTN) and 2 peptides from myosin heavy chain 6
206 (MYH6) (Fig.3f bottom panel, Supplementary Table 3).
207

208 **B cell-specific deletion of MHC II suppresses adverse cardiac remodeling after adoptive**
209 **transfer of post-MI splenic B cells.**

210 To then investigate B cell-dependent MHC II-mediated antigen presentation as a possible
211 mechanistic driver of adverse cardiac remodeling following ischemic myocardial injury, we used
212 transgenic mice with B cell-specific MHC II deletion ($Cd19^{tm1(cre)Cgn/-}H2\text{-}Ab1^{b\text{-tm1Koni}/\,b\text{-tm1Koni}}$) [25]
213 and repeated our adoptive transfer experiments (Fig.4a).

214

215 Four weeks following MI surgery, we performed adoptive transfer of splenic B cells from MHC
216 II-deficient HF mice into naïve wild-type (WT) mice. Flow cytometry analysis confirmed the
217 persistent absence of MHC II on donor B cells at the time of adoptive transfer (Supplementary
218 Fig.11). In a separate experiment, this time using CD45.1 mice as recipients, because the donor
219 MHC II-deficient and WT mice naturally express CD45.2, we confirmed the persistent presence
220 of donor B cells from MHC II-deficient mice 8 weeks following adoptive transfer (Supplementary
221 Fig.12). Adoptive transfer of splenic B cells from WT ischemic HF mice or sham-operated mice
222 served as positive and negative controls, respectively. Splenic B cells isolated from MHC II-
223 deficient mice with ischemic HF did not induce adverse cardiac remodeling upon adoptive transfer
224 as assessed by echocardiography (Fig.4b; mean LVEF 87.10±1.9% vs. 88.96±2.2% MHC II-
225 deficient HF vs. WT sham recipient, q = 0.11 at 8 weeks; mean LVESD 1.27±0.1mm vs.
226 1.19±0.1mm MHC II-deficient HF vs. WT sham recipient, q = 0.17 at 8 weeks). Gravimetric data
227 revealed borderline increases in cardiac mass and the absence of splenic hypertrophy following
228 the transfer of splenic B cells from MHC II-deficient HF mice (Fig.4c; spleen mean 2.86±0.3 vs.
229 2.83±0.2 mg/g MHC II-deficient HF vs. WT sham recipient, q = 0.83; heart mean 4.54±0.2 vs.
230 4.34±0.1 mg/g MHC II-deficient HF vs. WT sham recipient, q = 0.05). Cardiomyocyte
231 hypertrophy was also markedly reduced in recipients of splenic B cells from MHC II-deficient HF
232 mice compared to recipients of splenic B cells from WT HF mice (Fig.4d).

233

234 To reinforce the findings from the echocardiographic analysis, we performed proteomics analyses
235 of left ventricular samples from recipients of splenic B cells from WT sham, WT ischemic HF and
236 MHC II-deficient ischemic HF. This analysis confirmed adverse cardiac remodeling in recipients

237 of splenic B cells from WT HF mice relative to recipients from WT sham mice and highlighted
238 blunted adverse cardiac remodeling in recipients of splenic B cells from MHC II-deficient HF mice
239 (Fig.5a-b). There was significant upregulation of key proteins involved in adverse cardiac
240 remodeling (e.g. TPM and TNNT2), cell death and protein turnover (BAG3 and UBB) in recipients
241 of WT HF splenic B cells relative to MHC II-deficient HF splenic B cells. Interestingly, in
242 recipients of MHC II-deficient HF splenic B cells, there was significant upregulation of cardiac
243 repair/stabilization proteins in response to stress like MYOM1, GYG1, CCT2 and NID-1 (Fig.5c).
244

245 **Follicular splenic B cells mediate MHC II-dependent cardiac adverse remodeling post-MI**

246 We ran several control experiments to support proper interpretation of the results obtained using
247 MHC II-deficient B cells. First, we repeated the adoptive transfer experiment utilizing
248 *Cd19*$^{tm1(cre)Cgn/-I}$ mice as donors and confirmed that there were no off-target effects of the Cre
249 transgene (i.e. The results from these experiments were comparable to those using WT controls,
250 Supplementary Fig.13).
251

252 We then performed immunofluorescence to assess potential changes in serum antibodies targeting
253 myocardial proteins. We incubated heart sections from genetically B-cell deficient μMT mice with
254 serum collected from recipients of isolated splenic B cells from WT sham, WT HF and MHC II-
255 deficient HF mice 8 weeks post adoptive transfer and stained the histological sections with anti
256 IgG and IgM antibodies. We observed no differences in IgG-positive and IgM-positive stain
257 intensities across groups (Supplementary Fig.14).
258

259 Finally, we analyzed splenic B cells from MHC II-deficient ischemic HF (4 weeks post- MI) and

260 sham-operated mice. WT HF mice and sham-operated mice served as positive and negative
261 controls, respectively. We found that the deletion of MHC II on B cells was associated with an
262 increase in the percentage of follicular B cells and a decrease in marginal zone B cells post-MI
263 (Supplementary Fig.15). This raised the possibility that the deletion of MHC II on B cells might
264 suppress adverse cardiac remodeling post-adoptive transfer simply due to the decrease in marginal
265 zone B cells. We, therefore, repeated our adoptive transfer experiments, this time transferring
266 either follicular B cells or marginal zone B cells from HF or sham-operated mice (Fig.6a).
267
268 Splenic follicular B cells promoted adverse cardiac remodeling in naïve mice, evidenced by
269 reduction in LVEF and increase in LVESD relative to sham (Fig.6b); while marginal zone B cells
270 had no effect (Fig.6b). This identified splenic follicular B cells as the key mediators of adverse
271 cardiac remodeling along the cardio-splenic axis post-MI and reinforced a direct effect of B cell
272 MHC II deletion on B cell-dependent adverse cardiac remodeling post-MI.
273

274 **Single cell RNAseq based analysis indicates that adoptively transferred splenic B cells from**
275 **HF mice modulate myocardial T cells via an MHC-II dependent function.**

276 The results presented so far indicate that in ischemic HF, splenic B cells promote adverse cardiac
277 remodeling through an MHC II-dependent function, likely MHC II-mediated antigen presentation.
278 We used scRNA-seq to investigate the effect of adoptive transfer of splenic B cells from HF mice
279 on the cardiac immune cells of recipients. We isolated myocardial immune cells 8 weeks post-
280 adoptive transfer of splenic B cells from WT-HF, MHC II-deficient HF or WT sham operated mice
281 and analyzed them via scRNAseq (Fig.7a-b). We focused our analysis on T cell gene expressions
282 as B cells are known to present antigens to T cells. Comparative gene expression analysis of

283 recipients of splenic B cells from WT-HF vs WT sham operated mice revealed a list of 70 DEGs
284 in myocardial CD4 T cells (12 downregulated, 58 upregulated, adjusted $p<0.05$) and 745 DEGs in
285 myocardial CD8 T cells (6 downregulated, 739 upregulated, adjusted $p<0.05$, Supplementary
286 Table 4). When comparing recipients of MHC II-deficient HF splenic B cells to recipients of WT-
287 HF splenic B cells, we found minor differences in CD4 T cells, where 33 DEGs were upregulated
288 and 15 DEGS downregulated (adjusted $p<0.05$, Fig.7c, left bottom). The difference was more
289 pronounced in CD8 T cells in which only 2 genes were upregulated, and 84 genes were
290 downregulated (Fig.7c, right bottom; Supplementary Table 4). To gain insights into the biological
291 significance of these gene expression changes we used Ingenuity Pathways Analysis (IPA). IPA
292 showed that adoptive transfer of splenic B cells from HF mice resulted in upregulation of interferon
293 gamma (IFNγ) related signaling and other downstream signaling pathways in CD8 T cells
294 (Supplementary Fig.16). Depletion of MHC II from B cells resulted in downregulation of IFNγ
295 and STAT5B related signaling in CD8 T cells (Supplementary Fig.16). In CD4 T cells, IPA
296 showed that deletion of MHC II on B cells resulted in suppression of HSF1 mediated signaling, a
297 signaling pathway that drives the development of regulatory T cells [26].
298 Taken together, these observations suggest that post-MI splenic follicular B cells promote adverse
299 cardiac remodeling in ischemic heart failure through MHC II-dependent modulation of myocardial
300 T cells.
301

302 **Ischemic heart failure in humans is associated with differential expression of antigen**
303 **processing and presentation pathways in B cells.**
304 To evaluate the clinical relevance of our observations, we next sought to assess differentially
305 expressed biological pathways in B cells isolated from patients who experienced ischemic

306 myocardial injury. Since our murine data showed that changes in splenic B cells were reflected in
307 peripheral blood B cells (Supplementary Fig.7) and isolation of splenic B cells from patients was
308 not feasible, we performed a focused analysis of publicly available peripheral blood scRNAseq
309 data from patients with ST-elevation myocardial infarction (STEMI) [27] and patients with
310 established ischemic HF relative to healthy patients [28]. In both datasets, we identified peripheral
311 blood B cells and performed differential gene expression analysis.
312
313 The STEMI dataset included peripheral blood scRNAseq data of 38 patients 24-hours and 8-weeks
314 post-STEMI in addition to 38 healthy controls [27]. We performed DEG analysis within B cells,
315 comparing post-STEMI patients at both timepoints with healthy controls (Fig.8a). We identified
316 459 DEGs at 24-hours post-STEMI and 493 DEGs 8-weeks post-STEMI. KEGG pathway analysis
317 of these DEGs highlighted antigen processing and presentation as a differentially regulated
318 pathway both at 24-hours post-STEMI (q = 0.03) and 8-weeks post-STEMI (q = 0.03; Fig.8b),
319 with genes such as HLA-DRB5 and CIITA being differentially expressed and matching this
320 pathway. In the second dataset of three patients with established ischemic cardiomyopathy and
321 one matched healthy control (Fig.8c) [28], we identified 302 DEGs. Antigen processing and
322 presentation was identified here as a top differentially regulated pathway in patients with ischemic
323 HF (q = 2.09E-21; Fig.8d). DEGs relevant to these pathways included HLA-DRB1, HLA-DMA,
324 HLA-DQA1 and -DQA2, HLA-DQB1, which all encode for various MHC II proteins. Complete
325 lists of the DEGs within the antigen processing and presentation pathway are provided in
326 Supplementary Table 5.

327 **Discussion**

328 In this study, we report for the first time that splenic follicular B cells promote adverse cardiac

329 remodeling in ischemic heart failure. We show that splenic B cells present cardiac antigens on
330 MHC II molecules after MI and that their role in promoting adverse cardiac remodeling along the
331 cardio-splenic axis is largely dependent on MHC II. These findings change our understanding of
332 B cell biology in the post-MI period and point to B cell-mediated antigen presentation as a potential
333 novel and specific therapeutic target to prevent and treat ischemic heart failure.
334
335 Previous research has established that immune activation along the cardio-splenic axis is critical
336 in ischemic heart failure [7, 8, 29-32]. Although B cells are the most prevalent splenic immune
337 cell across multiple vertebrates, there is limited data on the role of B cells within the cardio-splenic
338 axis. To address this knowledge gap, we employed the adoptive transfer model developed by
339 Ismahil et al., which uniquely allows for the isolation of the functional effects of specific immune
340 cell types within the cardio-splenic axis of ischemic heart failure [8]. The adoptive transfer of
341 splenic B cells from mice with ischemic heart failure resulted in adverse cardiac remodeling with
342 evidence of persistent LV dilatation, reduced LV systolic function, and cardiomyocyte
343 hypertrophy in naïve mice. Our findings thus provide compelling evidence that B cells play a
344 significant role within the cardio-splenic axis of ischemic heart failure.
345
346 Our data corroborates previous observations regarding the dynamics of B cell transit to the heart
347 [10], in that adoptively transferred splenic B cells are re-distributed between the heart, spleen, and
348 peripheral blood of recipient mice, suggesting recirculation of transferred splenic B cells between
349 the heart and spleen. This does not exclude distribution to other organs, which has indeed been
350 described in prior studies in naïve mice [10]. The observation that MI triggered the differential
351 regulation of antigen processing and presentation pathways across splenic, myocardial and

352 circulating B cells further supports the notion that B cells actively recirculate between the spleen
353 and the heart through the peripheral blood after MI. Notably, the persistent unique gene expression
354 profile observed in B cells four weeks post-injury suggests that MI induces long-lasting alterations
355 in B cells even in the absence of observable changes in B cell frequency.
356
357 Analyzing the MHC-II associated peptidome of post-MI splenic B cells we found enrichment of
358 myocardial antigens. MYH-6, a protein that has been previously described as preferential target of
359 cardiotropic T cells in mice and humans [33, 34] was one of the strong MHC II binders detected,
360 at 2 distinct regions (two different MYH-6 peptides were identified as enriched). We did not
361 observe significant clonal expansion of B cells post-MI. We cannot exclude that this might be the
362 result of insufficient sequencing depth, yet there were no significant changes in the serum
363 concentration of cardiac autoantibodies. Data from the RITA-MI trial also suggests a lack of
364 autoantibody involvement, as serum immunoglobulin levels were not significantly changed from
365 time of MI (baseline) throughout B-cell depletion (Rituximab treatment) [35]. This does therefore
366 present the possibility that splenic B cells may acquire and present cardiac antigens through B cell
367 receptor (BCR)-independent mechanisms rather than through typical BCR engagement [36]. BCR-
368 independent, low-efficiency, antigen uptake has been well documented in B cells [37]. We
369 speculate that after an MI, release of high concentration of cardiac autoantigens might generate
370 appropriate conditions for BCR-independent antigen uptake. Our scRNA data highlights the
371 involvement of pattern recognition receptor (PRR) pathways; thus, there is a possibility that
372 activation of damage-associated molecular patterns (DAMPs) related mechanisms may be the
373 preceding step to loading of cardiac antigens on MHC II molecules of splenic B cells. Further
374 studies will be needed to understand in detail the mechanistic steps that lead to the loading of

375 myocardial antigens on MHC II molecules of splenic B cells.

376

377 The findings from our adoptive transfer experiments, which involved post-MI B cells with either
378 intact or deficient MHC II expression, underscore the importance of MHC II in mediating adverse
379 cardiac remodeling along the cardio-splenic axis. Specifically, the absence of MHC II led to a
380 reduction in adverse cardiac remodeling in recipient mice, as assessed by echocardiography,
381 gravimetric analysis, and mass spectrometry of myocardial tissue. While MHC II deletion can
382 influence various B cell functions, including survival, replication, and chemokine production, our
383 results suggest that MHC II-deficient B cells can survive after adoptive transfer and maintain
384 comparable frequencies in recipient animals relative to wild-type B cells. Notably, we found that
385 alterations in the composition of splenic B cells due to MHC II deletion did not account for the
386 phenotype observed in recipients of MHC II-deficient splenic B cells.
387 We cannot entirely rule out the impact of MHC II deletion on the secretion of B cell-specific
388 chemokines. This is a limitation of our study. Yet, collectively, our findings from the MHC-II
389 associated peptidome analysis and the experiments with MHC-II deficient B cells strongly suggest
390 that splenic B cells modulate adverse cardiac remodeling after MI through MHC II-dependent
391 antigen presentation. It bears emphasis that we noted mild effects of post-MI MHC II-deficient
392 splenic B cells, with trends toward increased cardiac mass, cardiomyocyte cross-sectional area,
393 (Figure 4 c,d) and mild changes at the proteomic level (Figure 5), indicating some degree of
394 adverse cardiac remodeling. This may stem from cytokine-dependent, MHC-II independent,
395 mechanisms by which B cells contribute to cardiac remodeling after MI [12, 38].

396

397 B cells typically present antigens via MHC II to CD4 T cells and, under specific conditions, CD8

398 T cells [39, 40], leading to T cell activation. Prior studies have implicated both CD4 and CD8 T
399 cells in adverse cardiac remodeling following myocardial injury [41-44]. In the present study, we
400 found that the adoptive transfer of splenic B cells from ischemic HF modulated gene expression
401 of both myocardial CD4 T cells and myocardial CD8 T cells in an MHC II dependent manner. In
402 the CD8 compartment, we observed MHC II dependent activation of IFNγ signaling, a key
403 mediator of immune mediated myocardial damage [45-47]. The downregulation of the mediator
404 STAT5B in the absence of MHC II further supports this dependency as altered STAT5B
405 expression and activation has been implicated in various cardiac pathologies [48, 49]. These
406 findings therefore suggest that adoptive transfer of post-MI splenic B cells triggers activation of
407 myocardial T cells, ultimately contributing to adverse cardiac remodeling. Notably, we observed
408 a stronger signal for MHC II dependent CD8 T cells activation, and minor changes in CD4 T cells.
409 It remains unclear whether this finding reflects a cascade of activation initiated by CD4 T cells
410 (with amplification of the activation along the signaling cascade) or if B cells independently
411 engage both CD4 and CD8 T cells, with a stronger effect on CD8 T cells. Further investigations
412 will be needed to clarify this interaction.
413
414 Our scRNAseq analyses of peripheral blood B cells from patients with ischemic myocardial injury
415 showed differential regulation of antigen processing and presentation in both the acute and chronic
416 post MI phases. Several genes involved in this pathway showed shared differential expression
417 between mice and humans, including multiple MHC complexes, CD74 (which stabilizes MHC II
418 molecules) [50], and HSPs, which are critical modulators of effector response post antigen
419 presentation [51, 52].This is noteworthy, as it points to a translational relevance of our findings.
420 However further work will be needed to assess the direct involvement of these conserved genes

421 and the extent to which B cell-mediated antigen presentation modulates adverse cardiac
422 remodeling in patients who experience an MI.
423
424 In summary, our findings reveal that MI triggers long-lasting changes in splenic B cells; that
425 splenic B cells present myocardial antigens via MHC II following myocardial infarction; and that
426 B cells circulating between the spleen and the heart drive post-MI adverse cardiac remodeling
427 through MHC II-mediated mechanisms. These observations not only expand our current
428 understanding of B cell biology but also reshape existing models of immune-cardiac interactions
429 post-myocardial injury [2, 53-55]. Moreover, they highlight the potential of targeting MHC II-
430 dependent B cell functions as a novel therapeutic approach to prevent and treat ischemic heart
431 failure. Further studies will be needed to understand whether our findings are relevant to other
432 conditions characterized by acute or chronic cardiac damage.

433 **Methods:**

434 All studies were approved by the Institutional Animal Care and Use Committee (ACUC) of the
435 Johns Hopkins University School of Medicine, under protocol numbers MO20M388 and
436 M023M238.
437

438 Mouse Models and Surgical Protocol:

439 Male 10-14- week-old mice were used for all experiments unless otherwise specified. All mice
440 were purchased from Jackson Laboratory (Bar Harbor, ME) or bred in the Johns Hopkins vivarium
441 facility. The following strains were used: C57BL/6J strain N. 000664, B6.SJL-*Ptprc*^{a} *Pepc*^{b}/BoyJ
442 (CD45.1) strain N. 002014, B6.129P2(C)-*Cd19*$^{tm1(cre)Cgn}$/J strain N. 006785, and B6.129X1-*H2-*
443 *Ab1*$^{b\text{-}tm1Koni}$/J strain N. 013181. To generate mice with B cell-specific MHC class II deletion,
444 B6.129P2(C)-*Cd19*$^{tm1(cre)Cgn}$/J and B6.129X1-*H2-Ab1*$^{b\text{-}tm1Koni}$/J mice were bred for target
445 *Cd19*$^{tm1(cre)Cgn/-}$*H2-Ab1*^{b}-tm1Koni/*b*-tm1Koni mice. Mice were randomly grouped into sham donors or HF
446 donors. HF donors underwent left thoracotomy with permanent ligation of the left anterior
447 descending (LAD) coronary artery to induce an MI. For the desired condition of ischemic HF,
448 mice were utilized at four weeks post- MI surgery [56, 57]. Sham donors underwent sham
449 intervention. Experiments referring to wildtype mice include a mix of heterozygous
450 *Cd19*$^{tm1(cre)Cgn/-}$*H2-Ab*$^{-/-}$, homozygous *Cd19*$^{tm1(cre)Cgn/-}$ littermate controls and syngeneic C57BL/6J
451 strain N. 000664.
452

453 Adoptive Transfer Studies:

454 Mice were euthanized four weeks following MI or sham surgery. Animals were gently perfused
455 through heart apex with 3mL Hanks' Balanced salt solution (HBSS) without $CaCl_2$, $MgCl_2$ or
456 $MgSO_4$ (GIBCO). Spleens were harvested and placed into a 35mm tissue culture dish with
457 phosphate-buffered saline (PBS). Splenocytes were isolated as previously published by Ismahil et
458 al [8]. Briefly, the spleen was minced finely using scissors and the end of a syringe plunger. The
459 solution was then pipetted through a 40µm cell strainer into a sterile 50mL tube. The tube was
460 centrifuged at 250g for 5 minutes at 4°C. After decanting the supernatant, the pellet was
461 resuspended with 5mL of ACK lysis buffer (Quality Biological) for 5 minutes at room temperature
462 to remove red blood cells (RBCs). After 5 minutes of lysis, 30mL of PBS was added to each tube
463 and each tube was centrifuged at 250g for 5 minutes at 4°C. The supernatant was decanted, and
464 pelleted splenocytes were then resuspended in sterile 0.9% sodium chloride for a final
465 concentration of ~$1x10^{8}$ total splenocytes in 150µL per retro-orbital injection into naïve recipient
466 mice.
467

468 For adoptive transfer studies with purified B cells, splenic B cells were isolated according to the
469 MojoSort™ Mouse Pan B Cell Isolation Kit protocol (BioLegend), with slight modifications.
470 Briefly, after mincing and filtering each spleen as described above, the pellet of each spleen was
471 resuspended with 4mL of Mojo buffer and then filtered again into fluorescence-activated cell
472 sorting (FACS) tubes. Each tube containing cells from one spleen was then centrifuged at 250g for
473 5 minutes at 4°C. After decanting the supernatant, the pellet was resuspended with cold 2mL Mojo
474 buffer. Samples were then incubated in 200µL of primary antibody cocktail for 15 minutes on ice,
475 followed by another 15 minutes incubation with 200µL of Nanobeads. Incubation was stopped
476 with 1.5mL Mojo buffer, and magnet sorted for 5 minutes. The cell suspension was decanted into

477 a fresh FACS tube, magnet incubation was repeated to increase the yield of isolated B cells. The
478 suspension of each spleen was then centrifuged, and each pellet was resuspended in FACS buffer.
479 The splenic B cell solutions from mice of the same experimental group were combined into a
480 single tube and then centrifuged prior to final resuspension in sterile 0.9% sodium chloride for
481 retro-orbital injection of ~$1x10^7$ splenic B cells in 150µL into naïve recipient mice. A small sample
482 was obtained pre- and post-antibody incubation to evaluate purity and yield by flow cytometry
483 (Supplementary Fig.1). Purified splenic B cells consistently had >95% purity.
484
485 For adoptive transfer studies with splenic B cell subtypes, single cell suspensions were prepared
486 as above and then stained with CD19-BV421, CD21-APC, and CD23-PE antibodies and
487 propidium iodide. Using MoFlo sorter, marginal zone B (MZB) cells and follicular B cells were
488 sorted as $CD19^+/CD21^+/CD23^{low}$ and $CD19^+/CD21^{low}/CD23^{high}$, respectively. Following
489 collection, samples from different mice were pooled, and all sorted and approximately $1.5x10^6$
490 MZB cells and $1x10^7$ follicular B cells were injected into naïve recipient mice, maintaining the
491 proportion of these two cell types in unfractionated splenocytes. These numbers of splenic B cell
492 subtypes were representative of the proportion relative to the total number of unsorted B cells from
493 a mouse spleen.
494

495 Echocardiography:

496 Mouse transthoracic echocardiography was performed in conscious mice prior to retro-orbital
497 injection to assess baseline cardiac structure and function, and again 4-, 8- and 16- weeks post
498 adoptive transfer. Echocardiography was performed using a VisualSonics Vevo 2100 Imaging
499 System. M-mode parasternal short images were obtained. LVEF and LVESD were measured using
500 Vevo Lab software v5.8.2.
501

502 Gravimetric and Histological Analyses:

503 Eight weeks after the adoptive transfer, recipient mice were euthanized, and hearts and spleens
504 were dissected and weighed. Tibia length and body weight were recorded to normalize the weights
505 of each mouse heart and spleen. Heart tissue was fixed with 10% neutral buffered formalin, -
506 embedded in paraffin, and stained with WGA using standard protocols.
507

508 Isolation of Myocardial Mononuclear Cells:

509 To analyze myocardial immune cells via flow cytometry, the heart was digested as previously
510 described with slight modifications [58]. Each heart was perfused with 3mL of Hank's Buffered
511 Salt Solution (HBSS) with calcium and magnesium infused into the left ventricle over 1 minute
512 with aortic clamping. Hearts were then dissected and cut transversely, approximately at the mid-
513 papillary muscle level, or approximately ~5mm below the atrioventricular groove. The superior
514 section was used for flow cytometry, and the apical section was used for histological analysis. The
515 heart tissue for flow cytometry was finely minced and 60mg was suspended in 3mL HBSS. Heart
516 tissue was digested with 300U DNAse, 625U collagenase II, and 50U hyaluronidase shaken for 30
517 minutes at 300rpm and 37°C. At the end of the 30 minutes, additional HBSS was added to each
518 tube to neutralize the enzymatic digestion. Each tube was then centrifuged at 250g for 5 min at
519 4°C. The supernatant was decanted, and the pellet was resuspended in 5mL of ACK lysis buffer
520 for 5 minutes at room temperature. The suspension was then diluted with PBS and filtered through

521 a 40μm strainer. Each cell suspension was centrifuged at 250g for 5 min prior to resuspension in
522 FACS buffer and filtering through a 35μm mesh strainer into a sterile FACS tube.
523

524 Isolation of Splenocytes for Flow Cytometry:

525 The spleens were removed and prepared as described above for adoptive transfer of splenocytes.
526 Following completion of RBC lysis, cells were resuspended in FACS buffer and filtered through
527 35μm cell strainers into sterile FACS tubes.
528

529 Isolation of Peripheral Blood Cells for Flow Cytometry:

530 Peripheral blood (~100μL) was collected via venipuncture of the facial vein into 1.5mL Eppendorf
531 tubes containing 100μL heparin. RBCs were lysed with 1mL ACK buffer for 5 minutes at room
532 temperature and then centrifuged at 250g for 5 minutes at 4°C. Cells were resuspended in 500μL
533 FACS buffer then filtered through 35μm cell strainers into FACS tubes.
534

535 Flow Cytometry:

536 Isolated cell suspensions were stained for 30 minutes on ice with the following fluorescently
537 conjugated antibodies: CD3-APC/Fire810 (clone 17A2, BioLegend), PD-1-BUV615 (clone
538 29F.1A12, BD Horizon), CD44-BV737 (clone IM7, Invitrogen), CXCR3-BV421 (clone CXCR3-
539 173, BioLegend), CD62L-BV510 (clone MEL-14, BioLegend), CD8 (clone 53-6.7, BioLegend),
540 CD69-BV650 (clone H1.2F3, BioLegend), CD27-BV785 (clone LG.3A10, BioLegend), KLRG-
541 1-PerCP/Cy5.5 (clone 2F1/KLRG1, BioLegend), CD103-PerCP/eFluor710 (clone 2E7,
542 Invitrogen), CXCR6-PE (cloneSA051D1, BioLegend), CD127-PE/Dazzle594 (clone A7R34,
543 BioLegend), ICOS-PE/Cy5 (clone 15F9, BioLegend), Ki-67-AF488 (clone SolA15, Invitrogen),
544 Granzyme B-Pacific Blue (clone GB11, BioLegend) CD25-BUV395 (clone PC61, BioLegend),
545 CD4-BV650 (clone GK1.5, BioLegend), CCR6-BV785 (clone29-2L7, BioLegend), CXCR5-
546 PerCP/eFluor710 (clone SPRCL5, Invitrogen), FOXP3-AF488 (clone MF-14, BioLegend),
547 CTLA-4-PE (clone UC10-4B9, BioLegend), T-bet-PE/Dazzle594 (clone 4B10, BioLegend),
548 RORrt-PE/Cy7 (clone Q31-378, BD Pharmingen) CD45-BUV395 (clone 30-F11, BD Horizon),
549 CD73-BV421 (clone TY/11.8, BioLegend), GL7-Pacific Blue (clone GL7, BioLegend), IgM-
550 BV605 (clone RMM-1, BioLegend), CD80-BV650 (clone 16-10A1, BioLegend), CD21/CD35-
551 BV711 (clone 7E9, BioLegend), CD19-BV750 (clone 6D5, BioLegend), I-ab-AF488 (clone KH-
552 74, BioLegend), CD5-PerCP (clone 53-7.3, BioLegend), CD1d-PerCP/Cy5.5 (clone L363,
553 BioLegend), CD23-PE (clone B3B4, BioLegend), CD86-PE/Dazzle594 (clone GL-1, BioLegend),
554 CD38-PE/Fire640 (clone 90, BioLegend), CD11b-PE/Cy5 (clone M1/70, BioLegend), PD-L2-
555 PE/Cy7 (clone TY25, BioLegend), CD138-PE/Fire810 (clone 281-2, BioLegend), CD93-APC
556 (clone AA4.1, BioLegend), IgD-APC/Fire 750 (clone 11-26c.2a, BioLegend) CD3-FITC (clone
557 17A2, Invitrogen), CD3-BV605 (17A2, BioLegend), CD19-BV421 (6D5, BioLegend), CD4-
558 Spark NIR 685 (GK1.5, BioLegend), CD8-BV785 (53-6.7, BioLegend), CD45-PerCP/Cyanine5.5
559 (30-F11, BioLegend), CCR2-APC (QA18A56, BioLegend), CD64-PE/Cy7 (X54-5/7.1,
560 BioLegend), Ly6C-BV650 (HK1.4, BioLegend), MHCII-BV711 (M5/114.15.2, BioLegend),
561 CD11b-Alexa Fluor 700 (M1/70, BioLegend), Ly6G-APC/Cy7 (1A8, BioLegend), CD45.1-PE
562 (A20, BioLegend). All antibodies were added at 1:1000 dilution for heart and spleen flow
563 cytometry and 1:500 for peripheral blood flow cytometry, with the following exceptions. PD-1

antibody was added at 1:1600 dilution. Ki-67, CXCR6, CD21/CD35, CD19, I-ab, and CD38 antibodies were added at 1:800 dilution. CD44, CD27, CD25, CTLA-4, and T-bet, PD-L2 antibodies were added at 1:100 dilution. Dead cells were excluded using the Zombie NIR dye (BioLegend) at 1:5000 dilution. Flow cytometry was performed on Cytek Aurora Full Spectrum Flow Cytometric Analyzer. Compensation controls were generated using single-color control samples and UltraComp eBeads (Invitrogen). Representative gating strategies are shown in individual figures.

Single Cell RNA (scRNA) Sequencing:

C57BL/6J mice 14-18 weeks-old underwent left thoracotomy with either sham surgery (n = 5) or permanent coronary LAD ligation (n = 11). Blood, heart, and spleen were collected 4 weeks post-sham or MI surgery ("heart failure"; n = 6) or 4 days post-MI surgery ("recent MI"; n = 5). For myocardial immune cell scRNA seq, recipient hearts (n=6/group) were collected 8 weeks after retro-orbital injections of splenic B cells from sham, HF or MHC II KO HF mice; half the heart, cut along the longitudinal axis were further processed for scRNAseq, remnant stored at -80°C. Single-cell suspensions for blood, heart, and spleen were prepared as described above. Heart and spleen samples were stained with 2 drops of Vibrant Dye Cycle Violet Ready Flow Reagent (DCV-Invitrogen) for 30 minutes, shaking at 300rpm and 37°C. Samples were stained with propidium iodide (PI), CD45-PE antibodies for all experiments and CD19-APC antibody for specific B cell subtypes, for 30 minutes on ice. Hashtag antibodies mapped to each experimental group were also added to cell suspensions at a concentration of 2μL per tube. B cells or $CD45^+$ cells were sorted using a MoFlo sorter. Equal numbers of the three experimental groups were mixed to reach a total of 20,000-30,000 cells that were combined in equal proportions within the same single cell library. Three libraries were prepared for the post-MI surgery experiment: 1) peripheral blood B cells; 2) splenic B cells; and 3) myocardial B cells. One library was prepared for the myocardial immune cell experiment.

Demultiplexing, barcode processing, single cell 5' gene counting, and V(D)J transcript sequence assembly and annotation were performed using Cell Ranger (10x Genomics). Gene specific analysis was performed using *Partek™ Flow™* software (v.11.0) for the post-MI surgery experiment and R (v.4.0.2) for myocardial immune cells experiment.

Uniform manifold approximation and projection (UMAP) plots were created on R (v.4.0.2) using Seurat (v.4.1.1) [59] standard parameters unless otherwise noted. Cells were filtered based on their distributions to only include those with 200-3200 unique features for blood, 200-3800 for heart (post-MI experiment), 200-4800 for heart (myocardial immune experiment), and 200-3500 for spleen, and < 8% mitochondrial read counts. Doublets not identified by hashtag demultiplex were removed using scDblFinder (v. 1.24.0). Counts were then logNormalized and scaled, and the top 2000 (post-MI experiment) and top 3000 (myocardial immune experiment) most variable genes were identified using the FindVariableFeatures function. Principal component (PC) analysis was performed using RunPCA and the first 15 PCs (post-MI) and 30 PCs (myocardial immune) were used to find the shared nearest neighbors (SNN) using the FindNeighbours function. Clustering was performed using the FindClusters function with a resolution of 0.2 and visualized using a UMAP projection. B cell and myocardial immune cell subtypes were classified using ScType [18] by using a modified list of known murine B cell and myocardial immune markers (Supplementary Table 6) and mapping mouse gene symbols to their human counterpart using biomart to be

compatible with ScType. Analyses of differential expressed genes between conditions per each cell type were performed using DEseq2 (1.46.0), with false-discovery rate (FDR) step-up used for multiple test corrections. Genes with low expression (<10 cells with 1 count) were filtered out prior to model fitting. For post-MI experiments lists of genes that exhibited differential expression based on the threshold of raw p-values<0.05 and log_2fold change >1 for upregulation of <-1 for downregulation were compiled and then analyzed against the Kyoto Encyclopedia of Genes and Genomes (KEGG) database on the Gene Set Enrichment Analysis (GSEA) website (https://www.gsea-msigdb.org; [19, 20]). Pathways were filtered using KEGG pathway annotations for immune-system specificity and were considered as differentially regulated if q-value from FDR was ≥ 0.05. For the myocardial immune experiment DEGs were filtered using threshold of adjusted p<0.05 and log_2fold change of ≥0.02 for upregulation and ≤-0.02 for downregulation. The functional analyses and networks were generated using QIAGEN IPA and IPA Interpret (QIAGEN Inc., https://digitalinsights.qiagen.com/IPA and https://digitalinsights.qiagen.com/products-overview/discovery-insights-portfolio/analysis-and-visualization/qiagen-ipa/qiagen-ipa-interpret/) [60].

The Chromium Next GEM Single Cell 5' Kit v2 (10x Genomics) was used to perform single cell transcriptional analyses. The Chromium Next GEM Single Cell V(D)J Kit was used to assess B cell receptor (BCR) cDNA and clonality. The Chromium Next GEM Single Cell V(D)J Kit was used to obtain BCR cDNA. Full-length and productive contigs were analyzed using scRepertoire (v.2.2.1). Only B cells with fully annotated heavy and light chains were kept for clonotype analysis. CDR3 nucleotide sequences plus V gene were used to define clonotypes. BCRs with >85% normalized Levenshtein distance of the nucleotide sequence were considered clones. All codes used for analyses is publicly available: https://github.com/caro471/Adamo_collaboration_2026.

Human scRNA Sequencing Analysis:

Publicly available scRNA sequencing data of peripheral blood from two cohorts were analyzed: three patients with ischemic cardiomyopathy (ICM) EGA accession: EGAS00001006330 [28] and 38 patients 24 hours and 8 weeks following ST segment elevation MI (STEMI) EGA accession: EGAD00001010064 [27] relative to healthy controls. These data were processed on R (v.4.0.2) using Seurat (v.4.1.1) as described above with the following modifications: Cells were filtered based on their distributions to only include those with 200-8000 unique features and <5% mitochondrial reads for the ICM dataset, 200 – 4500 unique features and <12% mitochondrial reads for the STEMI v2 dataset, 200 – 3500 unique features and <8% mitochondrial reads for the STEMI v3 dataset. 3000 variable features were used for both human datasets. Both datasets had notable batch effects that were corrected using Harmony [61]. For both datasets, the first 30 PCs were used for the SNN and clustering. A clustering resolution of 0.5 and 0.4 was used for the ICM and STEMI datasets respectively. B cells were identified using known human B cell-specific makers as previously described (Supplementary Table 6) [62]. For the larger dataset, B cells were pseudobulked per patient and differential gene expression was performed using DEseq2 controlling for sex and 10x chemistry in the regression model. Subsequent KEGG pathway analyses were performed as described above. For the smaller dataset, the defined threshold used was p-value <0.05, FDR step up <0.05and log_2fold change threshold of ≤-0.58 or ≥0.58 with p<0.05. For the larger dataset, a more stringent log_2fold change threshold of ≤-1 or ≥1 was used with p-value<0.05.

655

656 Peptidome Analysis:

657 Wildtype (WT) C57BL/6J and *Cd19*$^{tm1(cre)Cgn/-}$*H2-Ab1*$^{b\text{-tm1Koni}/\,b\text{-tm1Koni}}$ (MHC II-KO) mice (n = 16
658 total) underwent left thoracotomy with either sham surgery (n = 8) or permanent coronary ligation
659 (n = 8). MHC II KO mice were included to serve as negative controls. Four weeks following
660 surgery, spleens were collected from mice and splenic B cells were isolated, snap frozen in liquid
661 nitrogen, and stored at -80°C. Four spleens from the same experimental condition were combined
662 to get $2x10^6$ million B cells per experimental condition. Frozen splenic B cells were lysed and
663 purified for MHC-II bound peptides as previously described [63]. Briefly cells were lysed in
664 50mM Tris- 150mM NaCl buffer, supplemented with protease inhibitor cocktail (Roche) and 0.5%
665 NP-40 using a bead homogenizer. Lysates were cleared by centrifugation at 2000g and 4°C for 10
666 minutes, the supernatant was collected and cleared again by ultra-centrifugation at 100,000g and
667 4°C for 75 minutes. The supernatant was further cleared by flowing through Protein A/G
668 Sepharose column and then incubated for 2 hours at 4°C in Protein A/G Sepharose column cross-
669 linked with MHC-II mAb (M5/114.15.2, BioLegend) with slow agitation (60-80 rpm). Afterwards
670 flowthrough was decanted, and the peptide-bound column was washed four times: first with a
671 buffer containing, 0.05% NP-40, 50mM Tris, 150mM NaCl, 5mM EDTA, 0.1mM PMSF and
672 1mM Pepstatin A; second with 50mM Tris and 150mM NaCl; third 50mM Tris and 450mM NaCl
673 and finally 50mM Tris. Immuno-bound MHC molecules were then eluted with 10% acetic acid,
674 lyophilized and shipped to Dr Sidoli's lab and analyzed on an Orbitrap Fusion Lumos (Thermo
675 Scientific) mass spectrometer (details below).
676
677 Peptides abundances from WT groups were corrected using peptide abundances from MHC II-KO
678 mice, to eliminate background noise. The average abundance of corrected values was calculated
679 across technical replicates for each peptide. Peptides with mean corrected values above zero were
680 included in further analyses. The fold enrichment for each peptide was determined by dividing
681 values of HF group by sham. The binding affinity (BA) of these peptides were then determined
682 using the NetMHCIIpan-4.3 machine learning tool [64, 65]. Peptides with a fold enrichment of
683 greater than 1.2 and amino acid (AA) sequence length of 9 AAs were submitted into the BA server.
684 Briefly the server is trained on an extensive dataset of naturally occurring peptides covering
685 650,000 measurements of Binding Affinity and Eluted Ligand Mass spectrometry. The server
686 ranks each peptide according to predicted binding affinity in nanomolar IC50 compared against a
687 set of 100,000 random natural peptides [64, 65].
688

689 Cardiac proteomic sample preparation and analyses:

690 Snap frozen left ventricular tissue collected from recipients of adoptive transfer studies were
691 processed for mass spectrometry analyses using PreOmics® iST-NHS kit according to
692 manufacturer's instructions. Briefly, tissue was homogenized in LYSE-NHS buffer, sonicated and
693 boiled at 95°C for 10 minutes. Homogenates were cleared by centrifugation at 14,000g for 14
694 minutes, supernatant was collected, and samples were incubated in DIGEST buffer at 37°C for 1-
695 2 hours. Following digest, samples were labelled using TMTpro™ 16plex Label kit (Thermo
696 Fisher), washed, eluted, lyophilized and processed on an Orbitrap Fusion Lumos (Thermo
697 Scientific) mass spectrometer (details below).
698

699 Spectral TMT reporter ion intensities were quantified using the median sweep normalization
700 strategy originally described by Herbrich et al [66], following the implementation reported by
701 Foster et al [67], with minor modifications. Briefly, TMT reporter ion intensities were (1) log_2-
702 transformed, (2) median-centered within each channel, followed by (3) median-centering of each
703 individual spectrum across channels, and (4) protein abundance was determined by median
704 summarization, defined as the median of the log_2-transformed, median-centered intensities from
705 all spectra assigned to that protein within a given channel. Differential protein abundance between
706 experimental groups was evaluated using a Bayesian statistical framework implemented in linear
707 models for microarray data (LIMMA) with multigroup comparisons [68]. Pairwise contrasts were
708 also performed. Moderated p-values were adjusted for multiple testing using the positive false
709 discovery rate (q-value) approach described by Storey & Tibshirani [69]. Heat maps were
710 generated using the ComplexHeatmap R package with hierarchical clustering (Euclidean distance,
711 complete linkage). Principal component analysis (PCA) was performed using the PCAtools R
712 package. All codes used for statistical analysis, including PCA and heat map generation, is publicly
713 available at: https://github.com/Frostman300/MHCII_upload.
714

715 Mass Spectrometry:

716 Sample Desalting

717 Prior to mass spectrometry analysis of both TMT-labeled samples and peptides, samples were
718 desalted using a 96-well plate filter (Orochem) packed with 1 mg of Oasis HLB C-18 resin
719 (Waters). Briefly, the samples were resuspended in 100 µl of 0.1% TFA and loaded onto the HLB
720 resin, which was previously equilibrated using 100 µl of the same buffer. After washing with 100
721 µl of 0.1% TFA, the samples were eluted with a buffer containing 70 µl of 60% acetonitrile and
722 0.1% TFA and then dried in a vacuum centrifuge.
723

724 LC-MS/MS Acquisition and Analysis

725 Samples were resuspended in 10 µl of 0.1% TFA and loaded onto a Dionex RSLC Ultimate 300
726 (Thermo Scientific), coupled online with an Orbitrap Fusion Lumos (Thermo Scientific).
727 Chromatographic separation was performed with a two-column system, consisting of a C-18 trap
728 cartridge (300 µm ID, 5 mm length) and a picofrit analytical column (75 µm ID, 25 cm length)
729 packed in-house with reversed-phase Repro-Sil Pur C18-AQ 3 µm resin. Peptides were separated
730 using a 90 min gradient from 4-30% buffer B (buffer A: 0.1% formic acid, buffer B: 80%
731 acetonitrile + 0.1% formic acid) at a flow rate of 300 nl/min. The mass spectrometer was set to
732 acquire spectra in a data-dependent acquisition (DDA) mode from TMT-labeled samples and data-
733 independent mode (DIA) for peptidome samples. Briefly, the full MS scan was set to 300-1200
734 m/z in the orbitrap with a resolution of 120,000 (at 200 m/z) and an AGC target of 5x10e5. MS/MS
735 was performed in the Orbitrap using the top speed mode (2 secs), an AGC target of 2x10e5 and an
736 HCD collision energy of 45. Search tolerance for MS1 was 10ppm and 20ppm for MS2, fixed
737 modifications N-terminus TMT, lysine TMT and cysteine carbamidomethyl and methionine
738 oxidation set for variable modifications.

739 Proteome raw files were searched using Proteome Discoverer software (v2.5, Thermo Scientific)
740 using SEQUEST search engine and the SwissProt mouse database (updated April 2023). Any
741 peptide cleavage was specified for digestion, so that the software considered all protein fragments.
742 FDR determined by percolator validator. The mass spectrometry proteomics data have been

743 deposited to the ProteomeXchange Consortium via the PRIDE [70] partner repository with the
744 dataset identifier PXD073894
745

746 Immunofluorescence staining:

747 Endpoint serum from recipients of adoptive transfer studies were evaluated for cardiac
748 autoantibodies as previously described [71]. Briefly paraffin embedded cardiac cross-sections
749 from congenital B cell-deficient μMT mice were rehydrated and prepared using Tris-EDTA
750 antigen retrieval and incubated with recipient-serum (1:20 dilution) overnight at 4°C. Sections
751 were then washed and autoantibodies against cardiac antigens were then probed for using Biotin-
752 goat anti mouse IgG (clone Poly4053, BioLegend) and rat anti-mouse IgM (clone RMM-1,
753 BioLegend) at 1:1000 dilution. Following washes, the antibodies were detected using streptavidin-
754 Alexa555 (Invitrogen) and anti-rat-Alexa647 (Life Technologies); cardiomyocyte basement
755 membrane was stained with WGA-Alexa488 and nuclei stained with DAPI. Fluorescent images
756 were acquired using the PhenoImager™ HT 3.0, Vectra Polaris (Akoya Biosciences) slide scanner
757 at 40x objective, with the same exposure time. Images were processed using QuPath and analyzed
758 with ImageJ, three ROIs were taken for each section and two sections per sample. Aged mouse
759 serum was used for positive control and negative control were section without serum.
760

761 Statistical Analysis

762 Data was initially processed on Microsoft Excel (Microsoft 365). After assessing normality with
763 the Shapiro-Wilk test, Mann-Whitney or unpaired two-tailed t-tests were used for non-parametric
764 and parametric comparisons, respectively, of two groups. To compare data across three or more
765 groups, one-way analysis of variance (ANOVA) or Kruskal- Wallis tests were used for normally
766 distributed or non-Gaussian distributed data, respectively, followed by pairwise comparisons.
767 Serial echocardiographic data were analyzed using two-way ANOVA or mixed-effects analysis
768 followed by pairwise comparisons. WGA data were analyzed using nested t-test for two groups or
769 nested one-way ANOVA followed by pairwise multiple comparisons for three groups. All pairwise
770 multiple comparison tests were corrected using the original FDR method of Benjamini and
771 Hochberg. Outliers were determined using the ROUT method (Q=1%). All statistical tests were
772 performed on GraphPad Prism version 10.6.1 for Windows, GraphPad Software, Boston,
773 Massachusetts USA, www.graphpad.com.
774

Acknowledgments

The authors acknowledge the support for the Ross Flow Cytometry core funded by NIH Grant S10OD026859. The authors would also like to thank Dr. Edward Pearce for critical discussions and feedback on the manuscript and Dr. Hao Zhang from the Bloomberg FACS sorting Facility for technical support with FACS sorting. The Sidoli lab gratefully acknowledges for funding the Hevolution Foundation (AFAR), the Einstein-Rockefeller-CUNY-Mount Sinai Center for AIDS Research, the NIH Office of the Director (S10OD030286), and the Aging Biology Foundation.

Author contributions

OVE and JPL designed experiments, performed experiments, analyzed data, and wrote the manuscript. CD assisted with the analysis of murine and human scRNA data. SR, AB, YS, SS and KK assisted with collection and analysis of experimental data. KB, CC, SS, DBF, MM and SK helped with experimental design, review of data and manuscript edits. LA conceived the project, supervised experimental design and analyses, and wrote the manuscript with OVE and JPL.

References

1. Hofmann, U. and S. Frantz, *Immunity strikes: heart failure as a systemic disease.* Eur Heart J, 2014. **35**(6): p. 341-3.
2. Adamo, L., et al., *Reappraising the role of inflammation in heart failure.* Nat Rev Cardiol, 2020. **17**(5): p. 269-285.
3. Nahrendorf, M., et al., *The healing myocardium sequentially mobilizes two monocyte subsets with divergent and complementary functions.* J Exp Med, 2007. **204**(12): p. 3037-47.
4. Libby, P., M. Nahrendorf, and F.K. Swirski, *Leukocytes Link Local and Systemic Inflammation in Ischemic Cardiovascular Disease: An Expanded "Cardiovascular Continuum".* J Am Coll Cardiol, 2016. **67**(9): p. 1091-1103.
5. Murphy, S.P., et al., *Inflammation in Heart Failure: JACC State-of-the-Art Review.* J Am Coll Cardiol, 2020. **75**(11): p. 1324-1340.
6. Reina-Couto, M., et al., *Inflammation in Human Heart Failure: Major Mediators and Therapeutic Targets.* Front Physiol, 2021. **12**: p. 746494.
7. Swirski, F.K., et al., *Identification of splenic reservoir monocytes and their deployment to inflammatory sites.* Science, 2009. **325**(5940): p. 612-6.
8. Ismahil, M.A., et al., *Remodeling of the mononuclear phagocyte network underlies chronic inflammation and disease progression in heart failure: critical importance of the cardiosplenic axis.* Circ Res, 2014. **114**(2): p. 266-82.
9. Rocha-Resende, C., et al., *Developmental changes in myocardial B cells mirror changes in B cells associated with different organs.* JCI Insight, 2020. **5**(16).
10. Adamo, L., et al., *Myocardial B cells are a subset of circulating lymphocytes with delayed transit through the heart.* JCI Insight, 2020. **5**(3).
11. Bermea, K.C., et al., *The human myocardium harbors a population of naive B-cells with a distinctive gene expression signature conserved across species.* Front Immunol, 2022. **13**: p. 973211.
12. Zouggari, Y., et al., *B lymphocytes trigger monocyte mobilization and impair heart function after acute myocardial infarction.* Nat Med, 2013. **19**(10): p. 1273-80.
13. Adamo, L., et al., *Modulation of subsets of cardiac B lymphocytes improves cardiac function after acute injury.* JCI Insight, 2018. **3**(11).
14. Wu, L., et al., *IL-10-producing B cells are enriched in murine pericardial adipose tissues and ameliorate the outcome of acute myocardial infarction.* Proc Natl Acad Sci U S A, 2019. **116**(43): p. 21673-21684.
15. Heinrichs, M., et al., *The healing myocardium mobilizes a distinct B-cell subset through a CXCL13-CXCR5-dependent mechanism.* Cardiovasc Res, 2021. **117**(13): p. 2664-2676.
16. Schloss, M.J., et al., *B lymphocyte-derived acetylcholine limits steady-state and emergency hematopoiesis.* Nat Immunol, 2022. **23**(4): p. 605-618.
17. Adamo, L., C. Rocha-Resende, and D.L. Mann, *The Emerging Role of B Lymphocytes in Cardiovascular Disease.* Annu Rev Immunol, 2020. **38**: p. 99-121.
18. Ianevski, A., A.K. Giri, and T. Aittokallio, *Fully-automated and ultra-fast cell-type identification using specific marker combinations from single-cell transcriptomic data.* Nat Commun, 2022. **13**(1): p. 1246.

19. Mootha, V.K., et al., *PGC-1alpha-responsive genes involved in oxidative phosphorylation are coordinately downregulated in human diabetes.* Nat Genet, 2003. **34**(3): p. 267-73.
20. Subramanian, A., et al., *Gene set enrichment analysis: a knowledge-based approach for interpreting genome-wide expression profiles.* Proc Natl Acad Sci U S A, 2005. **102**(43): p. 15545-50.
21. Deffit, S.N. and J.S. Blum, *A central role for HSC70 in regulating antigen trafficking and MHC class II presentation.* Mol Immunol, 2015. **68**(2 Pt A): p. 85-8.
22. Houlihan, J.L., J.J. Metzler, and J.S. Blum, *HSP90alpha and HSP90beta isoforms selectively modulate MHC class II antigen presentation in B cells.* J Immunol, 2009. **182**(12): p. 7451-8.
23. Phan, U.T., B. Arunachalam, and P. Cresswell, *Gamma-interferon-inducible lysosomal thiol reductase (GILT). Maturation, activity, and mechanism of action.* J Biol Chem, 2000. **275**(34): p. 25907-14.
24. Sun, Y., et al., *Splenic Marginal Zone B Lymphocytes Regulate Cardiac Remodeling After Acute Myocardial Infarction in Mice.* J Am Coll Cardiol, 2022. **79**(7): p. 632-647.
25. Parker Harp, C.R., et al., *B cell antigen presentation is sufficient to drive neuroinflammation in an animal model of multiple sclerosis.* J Immunol, 2015. **194**(11): p. 5077-84.
26. Collins, C.B., et al., *Heat shock factor 1 drives regulatory T-cell induction to limit murine intestinal inflammation.* Mucosal Immunol, 2024. **17**(1): p. 94-110.
27. van Blokland, I.V., et al., *Single-Cell Dissection of the Immune Response After Acute Myocardial Infarction.* Circ Genom Precis Med, 2024. **17**(3): p. e004374.
28. Kuppe, C., et al., *Spatial multi-omic map of human myocardial infarction.* Nature, 2022. **608**(7924): p. 766-777.
29. Emami, H., et al., *Splenic metabolic activity predicts risk of future cardiovascular events: demonstration of a cardiosplenic axis in humans.* JACC Cardiovasc Imaging, 2015. **8**(2): p. 121-30.
30. van der Laan, A.M., et al., *Monocyte subset accumulation in the human heart following acute myocardial infarction and the role of the spleen as monocyte reservoir.* Eur Heart J, 2014. **35**(6): p. 376-85.
31. Kercheva, M., et al., *Characteristics of the Cardiosplenic Axis in Patients with Fatal Myocardial Infarction.* Life (Basel), 2022. **12**(5).
32. Ismahil, M.A., et al., *Splenic CD169 (+) Tim4 (+) Marginal Metallophilic Macrophages Are Essential for Wound Healing After Myocardial Infarction.* medRxiv, 2024.
33. Lv, H., et al., *Impaired thymic tolerance to α-myosin directs autoimmunity to the heart in mice and humans.* J Clin Invest, 2011. **121**(4): p. 1561-73.
34. Joachimbauer, A., et al., *Cardiopathogenic T Cells Govern Progression and Functional Remodeling in Inflammatory Cardiomyopathy and Chronic Myocarditis.* JACC Basic Transl Sci, 2026. **11**(2): p. 101458.
35. Zhao, T.X., et al., *Rituximab in patients with acute ST-elevation myocardial infarction: an experimental medicine safety study.* Cardiovasc Res, 2022. **118**(3): p. 872-882.
36. Rastogi, I., et al., *Role of B cells as antigen presenting cells.* Front Immunol, 2022. **13**: p. 954936.

880 37. Rock, K.L., B. Benacerraf, and A.K. Abbas, *Antigen presentation by hapten-specific B*
881 *lymphocytes. I. Role of surface immunoglobulin receptors.* J Exp Med, 1984. **160**(4): p.
882 1102-13.
883 38. Cohen, C.D., et al., *Myocardial Immune Cells: The Basis of Cardiac Immunology.* J
884 Immunol, 2023. **210**(9): p. 1198-1207.
885 39. Do, J.S., et al., *Unexpected role for MHC II-peptide complexes in shaping CD8 T-cell*
886 *expansion and differentiation in vivo.* Proc Natl Acad Sci U S A, 2012. **109**(31): p.
887 12698-703.
888 40. Migueles, S.A. and M. Connors, *Class II-Restricted CD8s: New Lessons Violate Old*
889 *Paradigms.* Immunity, 2016. **45**(4): p. 712-714.
890 41. Laroumanie, F., et al., *CD4+ T cells promote the transition from hypertrophy to heart*
891 *failure during chronic pressure overload.* Circulation, 2014. **129**(21): p. 2111-24.
892 42. Bansal, S.S., et al., *Activated T Lymphocytes are Essential Drivers of Pathological*
893 *Remodeling in Ischemic Heart Failure.* Circ Heart Fail, 2017. **10**(3): p. e003688.
894 43. Gröschel, C., et al., *T helper cells with specificity for an antigen in cardiomyocytes*
895 *promote pressure overload-induced progression from hypertrophy to heart failure.* Sci
896 Rep, 2017. **7**(1): p. 15998.
897 44. Santos-Zas, I., et al., *Cytotoxic CD8(+) T cells promote granzyme B-dependent adverse*
898 *post-ischemic cardiac remodeling.* Nat Commun, 2021. **12**(1): p. 1483.
899 45. Finger, S., et al., *A sequential interferon gamma directed chemotactic cellular immune*
900 *response determines survival and cardiac function post-myocardial infarction.*
901 Cardiovasc Res, 2019. **115**(13): p. 1907-1917.
902 46. Cosper, P.F., P.A. Harvey, and L.A. Leinwand, *Interferon-γ causes cardiac myocyte*
903 *atrophy via selective degradation of myosin heavy chain in a model of chronic*
904 *myocarditis.* Am J Pathol, 2012. **181**(6): p. 2038-46.
905 47. Levick, S.P. and P.H. Goldspink, *Could interferon-gamma be a therapeutic target for*
906 *treating heart failure?* Heart Fail Rev, 2014. **19**(2): p. 227-36.
907 48. Vaparanta, K., et al., *STAT5b is a key effector of NRG-1/ERBB4-mediated myocardial*
908 *growth.* EMBO Rep, 2023. **24**(5): p. e56689.
909 49. Jin, G., L. Wang, and J. Ma, *Inhibiting STAT5 significantly attenuated Ang II-induced*
910 *cardiac dysfunction and inflammation.* Eur J Pharmacol, 2022. **915**: p. 174689.
911 50. Schröder, B., *The multifaceted roles of the invariant chain CD74--More than just a*
912 *chaperone.* Biochim Biophys Acta, 2016. **1863**(6 Pt A): p. 1269-81.
913 51. Millar, D.G., et al., *Hsp70 promotes antigen-presenting cell function and converts T-cell*
914 *tolerance to autoimmunity in vivo.* Nat Med, 2003. **9**(12): p. 1469-76.
915 52. Barbera Betancourt, A., et al., *T Cell-Mediated Chronic Inflammatory Diseases Are*
916 *Candidates for Therapeutic Tolerance Induction with Heat Shock Proteins.* Front
917 Immunol, 2017. **8**: p. 1408.
918 53. Frangogiannis, N.G., *The inflammatory response in myocardial injury, repair, and*
919 *remodelling.* Nat Rev Cardiol, 2014. **11**(5): p. 255-65.
920 54. Westman, P.C., et al., *Inflammation as a Driver of Adverse Left Ventricular Remodeling*
921 *After Acute Myocardial Infarction.* J Am Coll Cardiol, 2016. **67**(17): p. 2050-60.
922 55. Rurik, J.G., H. Aghajanian, and J.A. Epstein, *Immune Cells and Immunotherapy for*
923 *Cardiac Injury and Repair.* Circ Res, 2021. **128**(11): p. 1766-1779.
924 56. Yang, F., et al., *Myocardial infarction and cardiac remodelling in mice.* Exp Physiol,
925 2002. **87**(5): p. 547-55.

57. Lindsey, M.L., et al., *Guidelines for in vivo mouse models of myocardial infarction.* Am J Physiol Heart Circ Physiol, 2021. **321**(6): p. H1056-h1073.
58. Bermea, K.C., S.T. Rousseau, and L. Adamo, *Flow Cytometry-Based Quantification and Analysis of Myocardial B-cells.* J Vis Exp, 2022(186).
59. Hao, Y., et al., *Integrated analysis of multimodal single-cell data.* Cell, 2021. **184**(13): p. 3573-3587.e29.
60. Krämer, A., et al., *Causal analysis approaches in Ingenuity Pathway Analysis.* Bioinformatics, 2014. **30**(4): p. 523-30.
61. Korsunsky, I., et al., *Fast, sensitive, and accurate integration of single cell data with Harmony.* bioRxiv, 2018: p. 461954.
62. Bermea, K.C., et al., *Myocardial B cells have specific gene expression and predicted interactions in dilated cardiomyopathy and arrhythmogenic right ventricular cardiomyopathy.* Front Immunol, 2024. **15**: p. 1327372.
63. Purcell, A.W., S.H. Ramarathinam, and N. Ternette, *Mass spectrometry-based identification of MHC-bound peptides for immunopeptidomics.* Nat Protoc, 2019. **14**(6): p. 1687-1707.
64. Reynisson, B., et al., *Improved Prediction of MHC II Antigen Presentation through Integration and Motif Deconvolution of Mass Spectrometry MHC Eluted Ligand Data.* J Proteome Res, 2020. **19**(6): p. 2304-2315.
65. Nilsson, J.B., et al., *Accurate prediction of HLA class II antigen presentation across all loci using tailored data acquisition and refined machine learning.* Sci Adv, 2023. **9**(47): p. eadj6367.
66. Herbrich, S.M., et al., *Statistical inference from multiple iTRAQ experiments without using common reference standards.* J Proteome Res, 2013. **12**(2): p. 594-604.
67. Foster, D.B., et al., *Integrated Omic Analysis of a Guinea Pig Model of Heart Failure and Sudden Cardiac Death.* J Proteome Res, 2016. **15**(9): p. 3009-28.
68. Smyth, G.K., *Linear models and empirical bayes methods for assessing differential expression in microarray experiments.* Stat Appl Genet Mol Biol, 2004. **3**: p. Article3.
69. Storey, J.D. and R. Tibshirani, *Statistical significance for genomewide studies.* Proc Natl Acad Sci U S A, 2003. **100**(16): p. 9440-5.
70. Perez-Riverol, Y., et al., *The PRIDE database at 20 years: 2025 update.* Nucleic Acids Res, 2025. **53**(D1): p. D543-d553.
71. Ramos, G.C., et al., *Myocardial aging as a T-cell-mediated phenomenon.* Proc Natl Acad Sci U S A, 2017. **114**(12): p. E2420-e2429.

962 **Figure Legends**

Fig. 1.

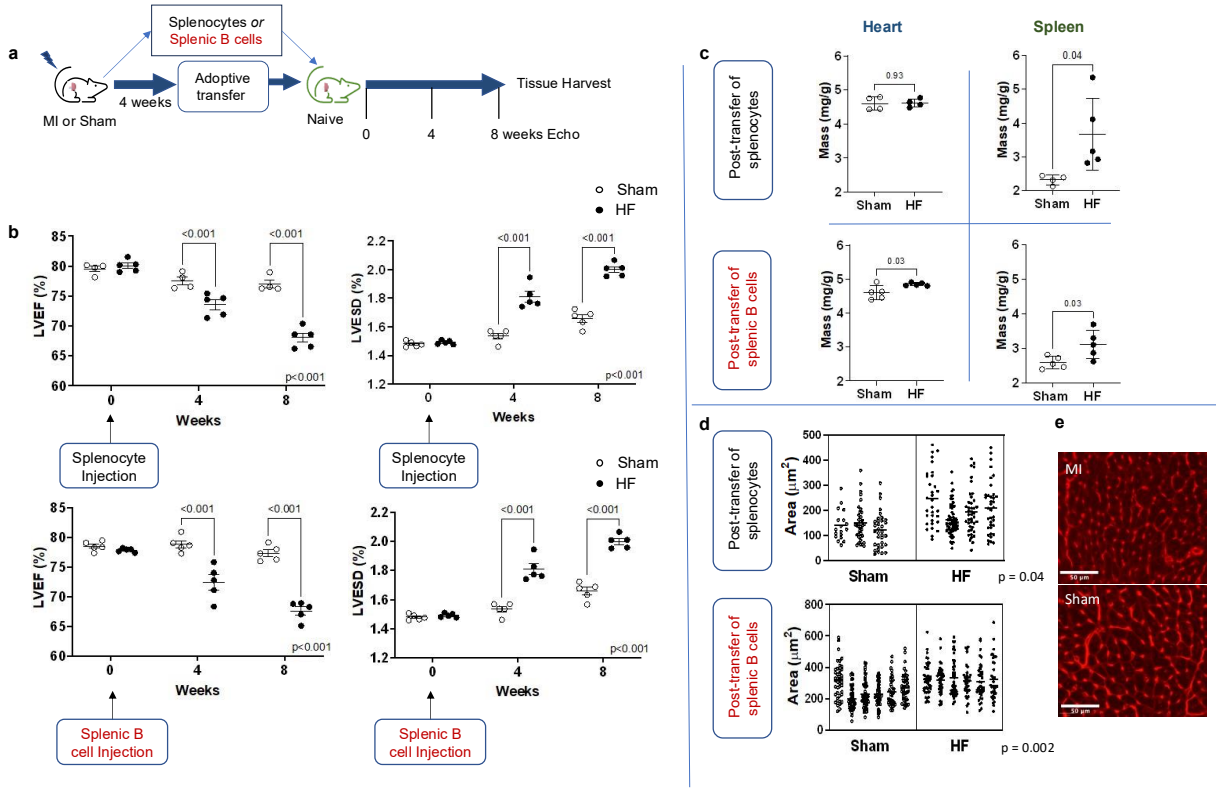

963

964 **Fig.1: Splenic B cells promote adverse cardiac remodeling in ischemic heart failure a**)
965 Schema for adoptive transfer studies. Four weeks following permanent LAD coronary ligation or
966 sham surgery, unfractionated splenocytes or isolated splenic B cells were transferred to naïve
967 recipient mice. Recipient mice underwent serial transthoracic echocardiography over 8 weeks
968 followed by tissue harvest. **b**) On echocardiography, adoptive transfer of splenocytes or isolated
969 splenic B cells from heart failure (HF) mice resulted in significant reduction in left ventricular
970 ejection fraction (LVEF) and increase in left ventricular end-systolic diameter (LVESD) in naïve
971 recipient mice. **c**) Quantitative gravimetric data revealed significantly larger hearts and spleens
972 (normalized to body weight) in naive mice 8 weeks post-adoptive transfer of splenocytes or
973 isolated splenic B cells from HF mice relative to recipients of splenocytes or splenic B cells from
974 sham-operated mice. **d**) Cardiomyocyte area was increased in recipients of splenocytes or isolated
975 splenic B cells from HF mice relative to sham recipients; n = 5-6 mice per group. Mean values ±
976 SD are represented. **e**) Representative images of WGA staining of hearts from recipients of isolated
977 splenic B cells from HF or sham-operated mice. LAD- left anterior descending. HF-heart failure.

978

Fig. 2.

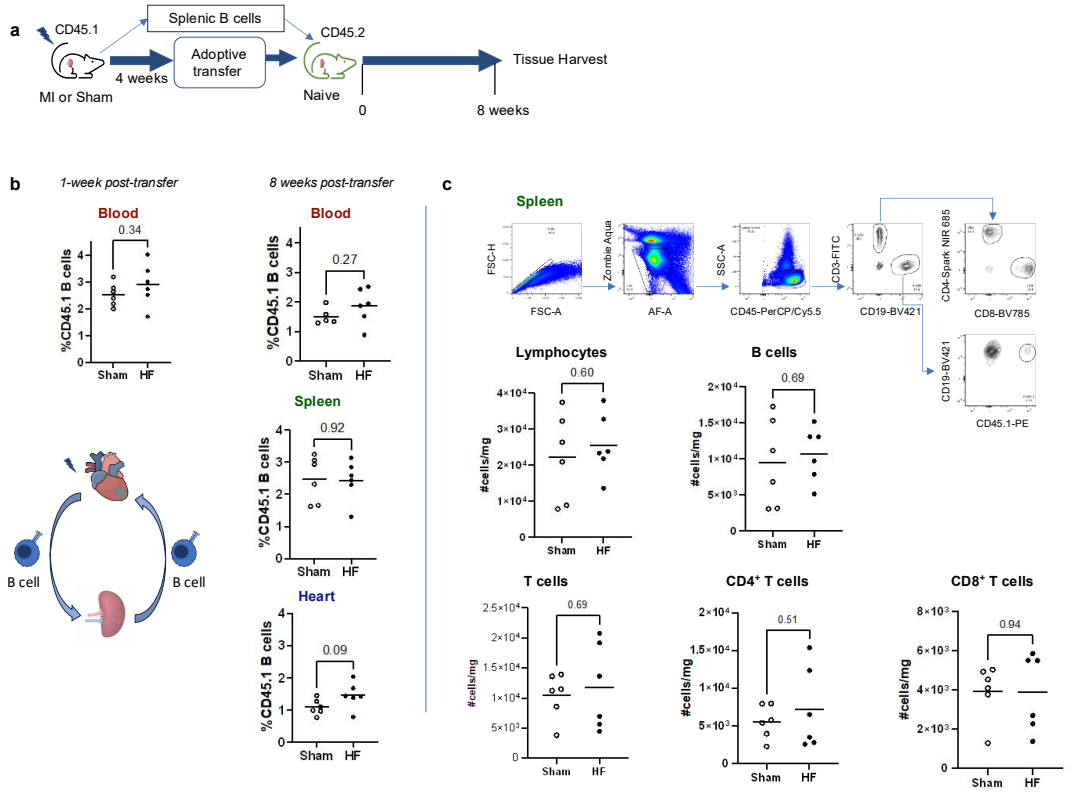

Fig.2: Adoptively transferred splenic B cells from mice with ischemic HF are found in the heart and spleen of recipients, and do not alter the immune composition of the spleen of naïve mice a) Schema for adoptive transfer of isolated splenic CD45.1 B cells 4 weeks following LAD ligation or sham surgery to naïve CD45.2 mice. **b**) Flow cytometry of peripheral blood from naïve recipient mice revealed the presence of donor CD45.1 B cells 1 week and 8 weeks following adoptive transfer. Donor CD45.1 B cells were also present in the spleen and heart of CD45.2 mice 8 weeks after adoptive transfer. **c**) Representative gating strategy for flow cytometry of spleens from recipient mice 8 weeks post-adoptive transfer of splenic B cells. Adoptive transfer of splenic B cells from HF mice had no effect on total number of lymphocytes, B cells, $CD4^+$ and $CD8^+$ T cells relative to recipients of sham splenic B cells. LAD- left anterior descending. HF-heart failure. n = 6 mice per group. Mean values are represented.

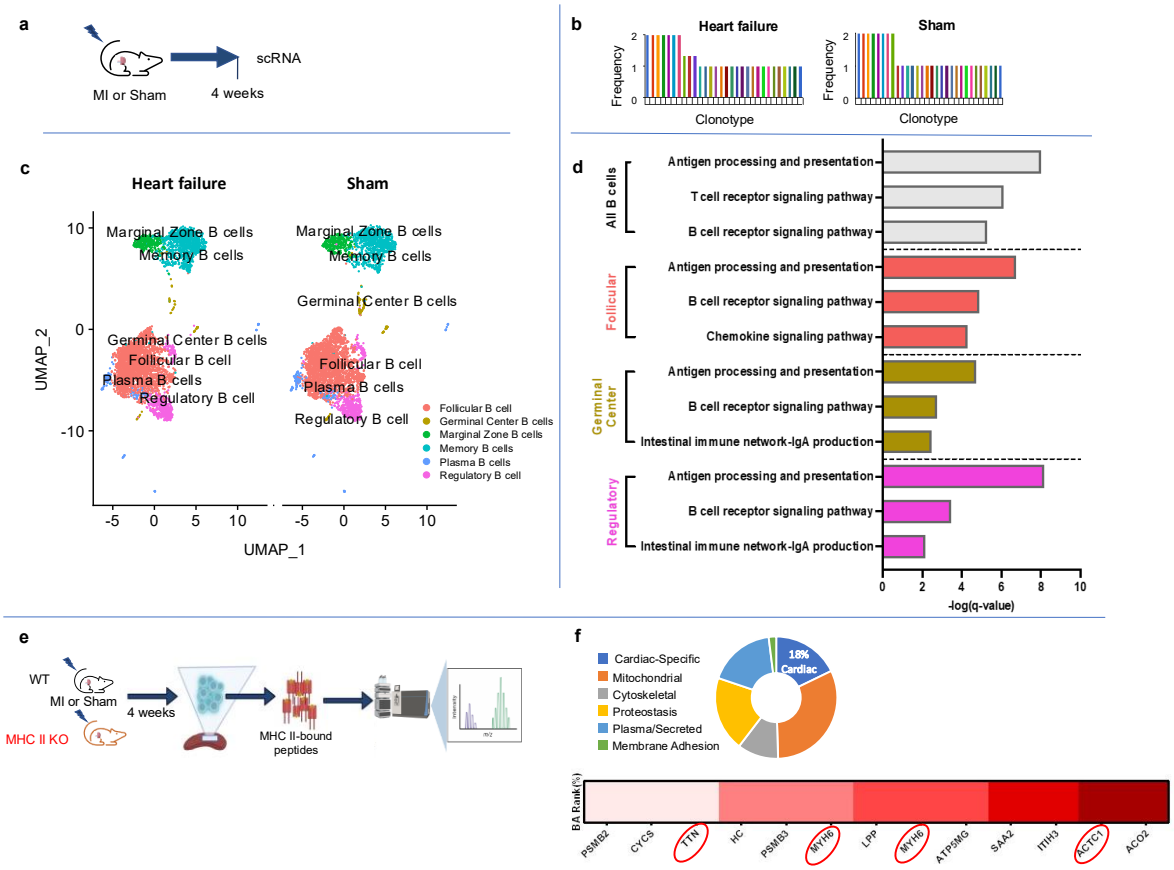

Fig. 3.

Fig.3: Ischemic myocardial injury is associated with activation of antigen processing and presentation pathways in splenic B cells and with enrichment of myocardial peptides within the MHC-II molecules of these B cells a) Schema for single cell sequencing of splenic B cells from mice 4 weeks following permanent LAD coronary ligation or sham surgery. **b**) V(D)J analysis of splenic B cells. Ischemic myocardial injury did not induce splenic B cell clonal expansion. **c**) UMAP plots of splenic B cells from heart failure or sham surgery mice. Splenic B cells were classified into B cell sub-types. **d**) KEGG pathway analysis of differentially expressed genes in splenic B cells (fold change >1, $p<0.05$) revealed significant differential expression of antigen processing and presentation in multiple B cell sub-types, post-MI. All pathways with FDR <0.05 are listed. (n = 4-5 mice per group). **e**) Schema for mass spectrometry of MHC-II bound peptides from splenic B cells four weeks after permanent LAD coronary ligation or sham surgery. Splenic B cells from MHC II KO (*Cd19tm1(cre)Cgn/-H2-Ab1b*-tm1Koni/ *b*-tm1Koni) mice were included besides cells from WT (wildtype) mice to allow identification of background signal. **f**) Categories of proteins both enriched > 1.2 folds in the MHC-II molecules of splenic B cells isolated from mice with ischemic HF and *in silico* confirmed binding to the C57Bl/6 specific MHC-II molecule H2-I-Ab. 18% of these proteins are cardiac-specific. The peptides/corresponding proteins identified as strong binders are reported in the heat map. The cardiac proteins titin (TTN), myosin heavy chain 6 (MYH6) and α-actin (ACTC1) were identified among the top predicted

strong binding peptides. MYH-6 is repeated twice because two different peptides from MYH-6 were detected. LAD- left anterior descending. HF-heart failure.

Fig. 4.

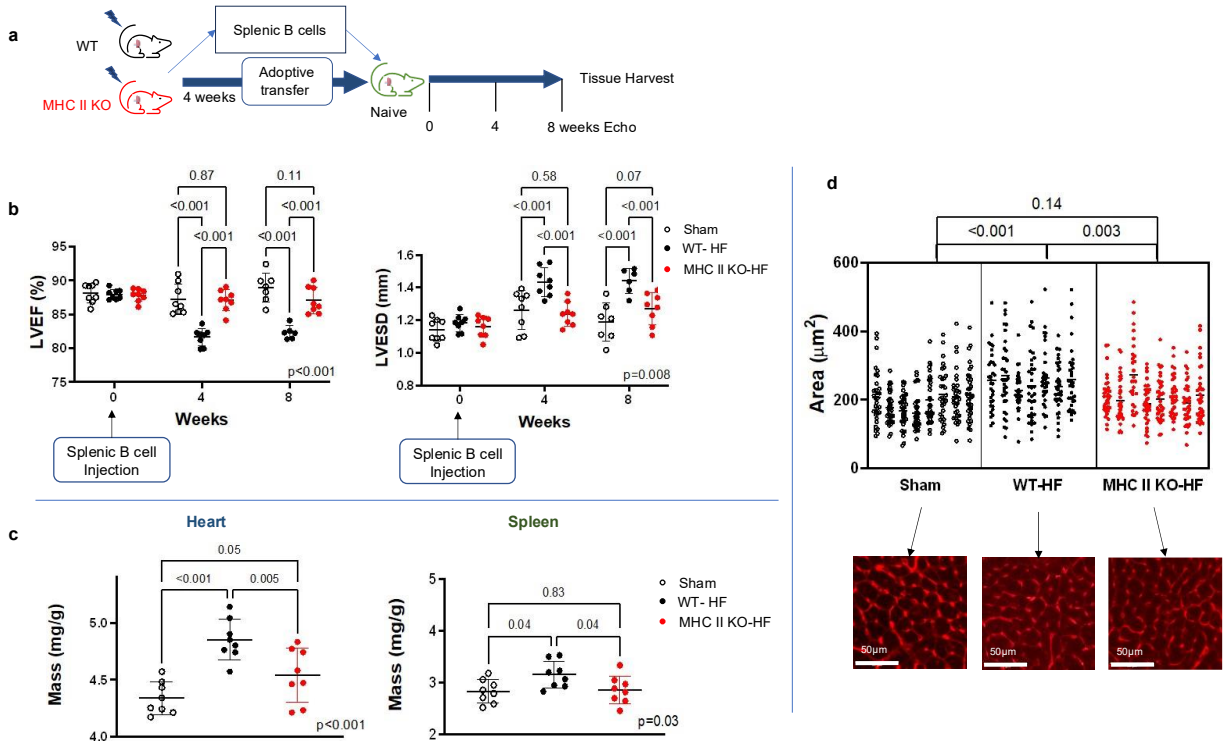

Fig.4: Transfer from ischemic HF mice of splenic B cells deficient in MHC class II does not produce adverse cardiac remodeling in naïve recipient mice at the echocardiographic, gravimetric or histological level a) Schema for adoptive transfer studies of isolated splenic B cells from *Cd19tm1(cre)Cgn/-H2-Ab1b*-tm1Koni/ *b*-tm1Koni mice and wildtype mice following permanent LAD coronary ligation or sham surgery. **b**) Naïve recipients of splenic B cells isolated from HF mice with B cell-specific MHC class II deletion did not experience adverse cardiac remodeling on serial echocardiography over an 8-week period post-adoptive transfer. **c**) Gravimetric data of recipient mice. Recipient mice of B cells deficient in MHCII from HF mice did not experience significant splenic or cardiac remodeling by gravimetric analysis. **d**) Representative images of WGA staining of hearts from recipient mice. Transfer of isolated MHCII-deficient splenic B cells did not induce cardiomyocyte hypertrophy. LAD- left anterior descending. HF-heart failure. n= 8 mice per group. Mean values ± SD are represented.

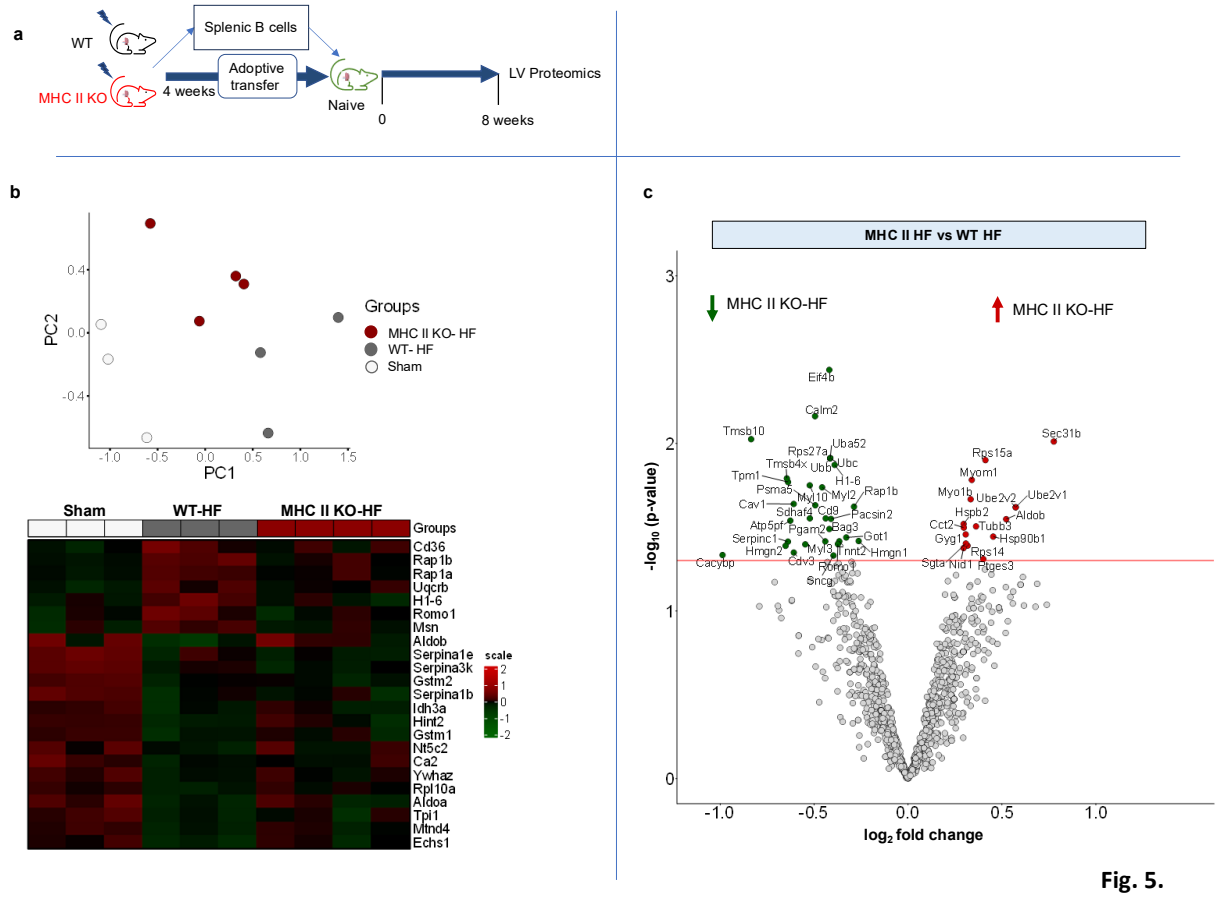

Fig. 5.

Fig.5: Mass spectrometry of left ventricle shows that transfer of splenic B cells from mice with ischemic HF into naïve recipients results in adverse cardiac remodeling, which is blunted when splenic B cells are deficient in MHC class II **a**) Schema for adoptive transfer studies of isolated splenic B cells from *Cd19tm1(cre)Cgn/-H2-Ab1b*-tm1Koni/*b*-tm1Koni mice and wildtype (WT) mice following permanent coronary artery ligation or sham surgery. LV-Left ventricle. **b**) PCA plot of protein clusters within each animal across the three groups and heatmap of proteins significantly changed between WT heart failure (WT-HF) and sham. Transfer of isolated MHC II-deficient splenic B cells from heart failure mice (MHC II KO-HF) shifts cardiac proteome of naïve recipients towards control. **c**) Volcano plot of proteomics comparison between WT and MHC II-deficient heart failure recipient mice. Protein markers of adverse cardiac remodeling are down regulated in naïve recipients of heart failure MHC II-deficient splenic B cells relative to wildtype recipients. n=3-4 mice per group. LIMMA statistical test.

Fig. 6.

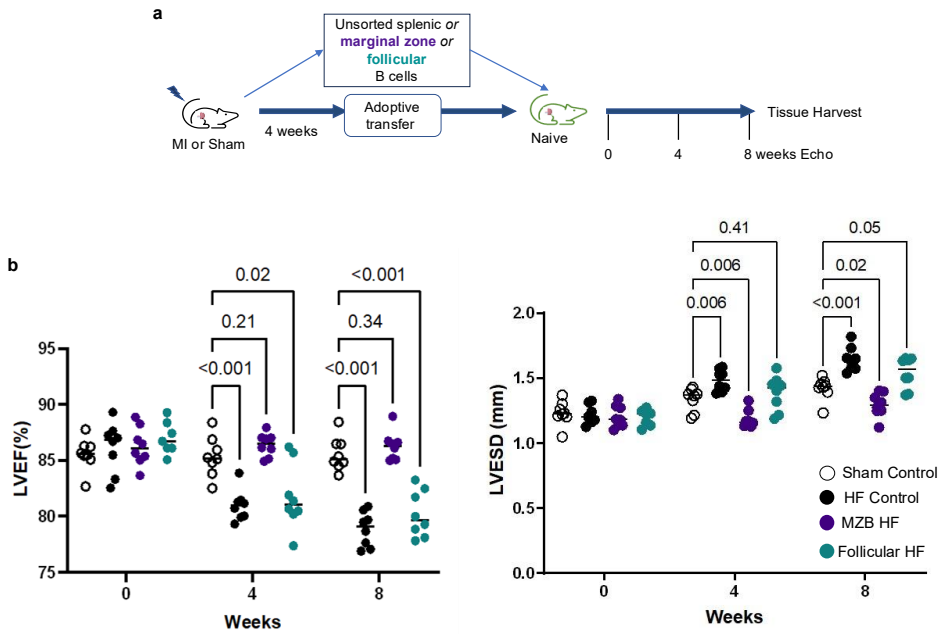

Fig.6: Splenic Follicular B cells promote adverse cardiac remodeling in ischemic HF a) Schema for adoptive transfer studies. Four weeks following permanent LAD coronary ligation, follicular splenic B cells or marginal zone splenic B (MZB) cells were transferred to naïve recipient mice. The adoptive transfer of unsorted splenic B cells from mice 4 weeks following coronary artery ligation (HF control) or sham surgery served as positive and negative controls, respectively. Recipient mice underwent serial transthoracic echocardiography over 8 weeks. **b**) On echocardiography, adoptive transfer of splenic follicular B cells from heart failure (HF) mice resulted in a reduction in left ventricular ejection fraction (LVEF) ($p<0.001$) and an increase in left ventricular end-systolic diameter (LVESD) in naïve recipient mice over eight weeks ($p=0.05$) compared to recipients of splenic B cells from sham-operated mice. The adoptive transfer of marginal zone B cells from HF mice did not result in LVEF reduction or LV dilatation. n = 8 mice per group. Mean values ± SD are represented.

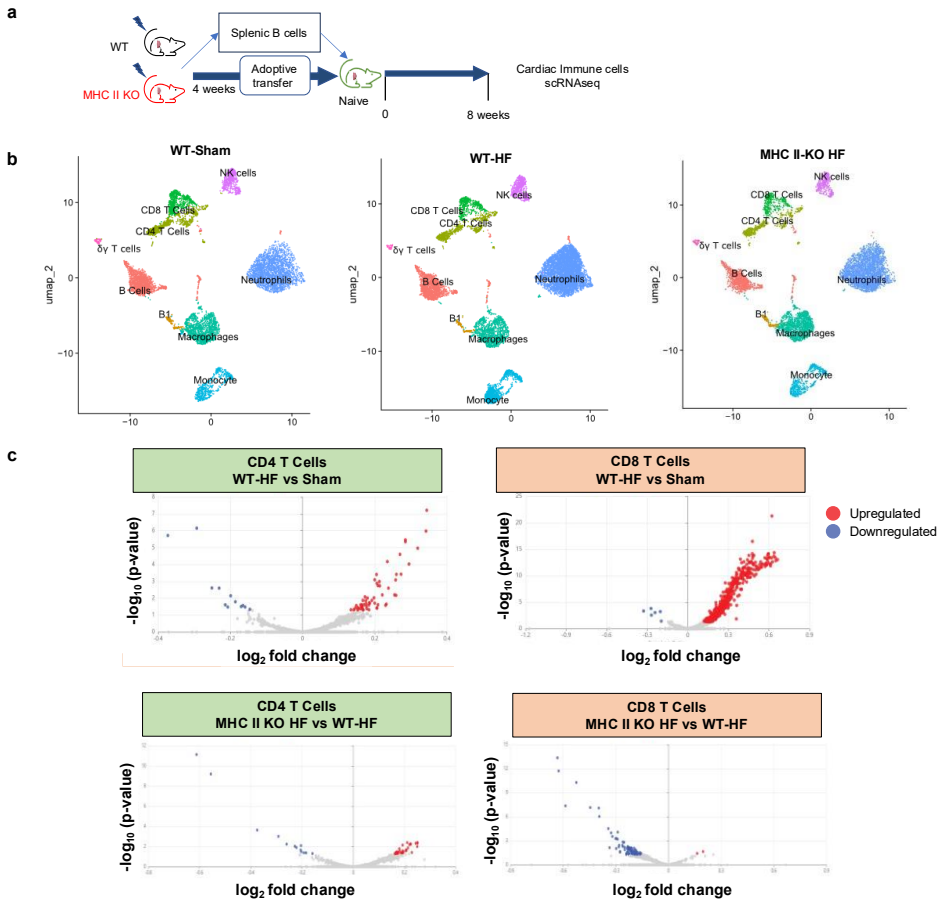

Fig. 7.

Fig.7: Adoptive transfer of splenic B cells from mice with ischemic HF produces MHC-II dependent changes in myocardial T cells 8 weeks post transfer **a**) Schema for scRNA-seq based analysis of chronic changes in myocardial immune cells mediated by splenic B cells in the context of ischemic HF. 4 weeks post-MI splenic B cells from WT or *Cd19tm1(cre)Cgn/-H2-Ab1b*-tm1Koni/ *b*-tm1Koni (MHC II KO) mice were isolated and transferred into naïve recipients. 8 weeks later myocardial immune cells were isolated from recipient animals and analyzed via scRNA-seq. **b**) UMAP plots of myocardial immune cells 8 weeks post adoptive transfer of splenic B cells from WT sham, WT HF or MHC II deficient HF mice. **c**) Ingenuity Pathway Analysis (IPA) generated volcano plots of significantly differentially expressed genes; adjusted $p<0.05$, (n = 6 mice per group). HF= heart failure.

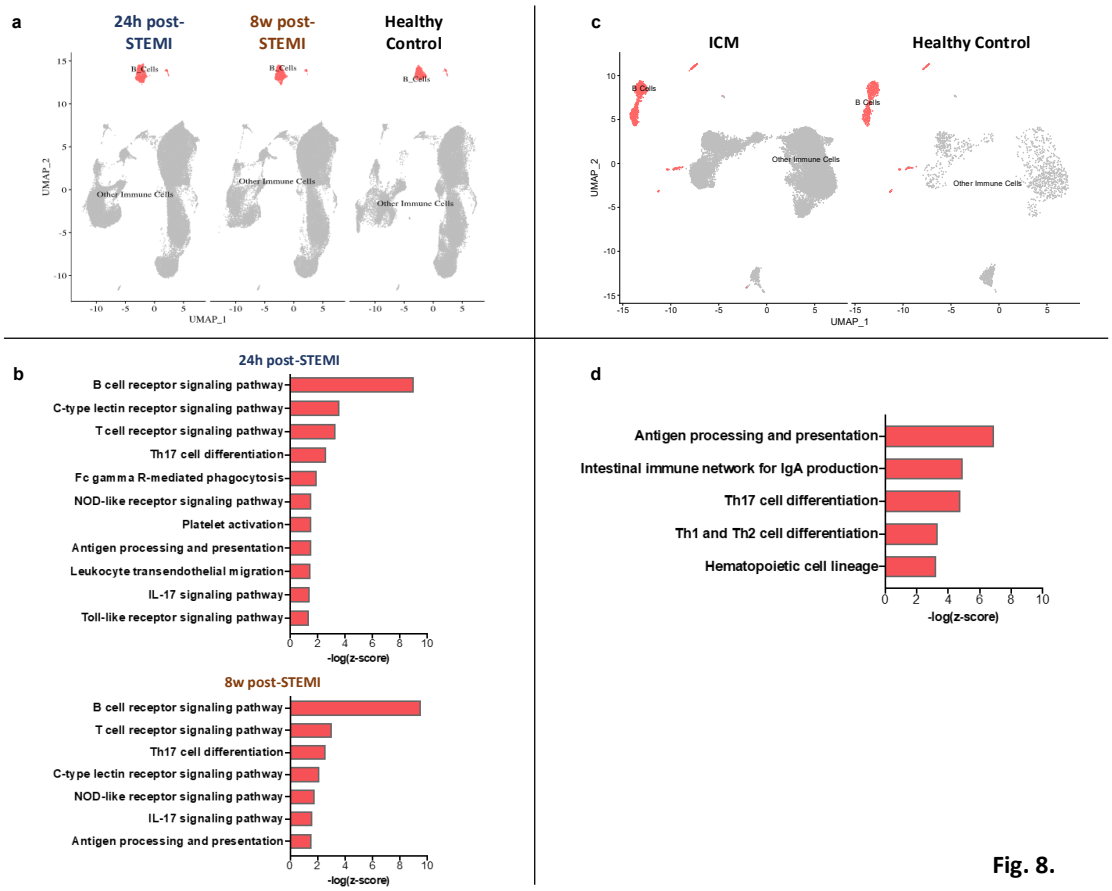

Fig. 8.

Fig.8: Antigen processing and presentation is differentially expressed in circulating B cells in humans post-STEMI or with ischemic cardiomyopathy **a**) Single cell sequencing of peripheral blood B cells from 38 patients 8-weeks or 24-hours post-STEMI and 38 healthy controls. UMAP plots are shown with B cells identified. **b**) KEGG pathway analysis of differentially expressed genes ($\log_2$foldchange$\leq$-1$\geq$1, $p<0.05$) revealed significant differential regulation of antigen processing and presentation in peripheral B cells of patients at both 24 hours and 8 weeks post STEMI. **c**) Single cell sequencing of peripheral blood B cells from 3 patients with ischemic cardiomyopathy (ICM) and 1 healthy patient. UMAP plots are shown with B cells identified. **d**) KEGG pathway analysis of differentially expressed genes ($\log_2$foldchange$\leq$-0.58$\geq$0.58, FDR<0.05, $p<0.05$) revealed significant differential expression of antigen processing and presentation in peripheral blood B cells from ICM patients. All immune system pathways with FDR <0.05 are listed. Th = T helper. NOD = nucleotide oligomerization domain. IL = interleukin.